Published in final edited form as:
Bioorg Med Chem. 2013 February 15; 21(4): 891–902. doi:10.1016/j.bmc.2012.12.010.

Synthesis of N^4-(Substituted phenyl)-N^4-alkyl/desalkyl-9*H*-pyrimido[4,5-*b*]indole-2,4-diamines and Identification of New Microtubule Disrupting Compounds that are Effective against Multidrug Resistant Cells1

Aleem Gangjee[a,*,†], **Nilesh Zaware**[a], **Ravi Kumar Vyas Devambatla**[a], **Sudhir Raghavan**[a], **Cara D. Westbrook**[b], **Nicholas F. Dybdal-Hargreaves**[b], **Ernest Hamel**[c], and **Susan L. Mooberry**[b,*,†]

[a]Division of Medicinal Chemistry, Graduate School of Pharmaceutical Sciences, Duquesne University, 600 Forbes Avenue, Pittsburgh, PA15282, USA

[b]Department of Pharmacology, University of Texas Health Science Center at San Antonio, and Cancer Therapy & Research Center, 7703 Floyd Curl Drive, San Antonio, TX 78229, USA

[c]Screening Technologies Branch, Developmental Therapeutics Program, Division of Cancer Treatment and Diagnosis, National Cancer Institute, Frederick National Laboratory for Cancer Research, National Institutes of Health, Frederick, MD 21702, USA

Abstract

A series of fourteen N^4-(substituted phenyl)-N^4-methyl/desmethyl-9*H*-pyrimido[4,5-*b*]indole-2,4-diamines was synthesized as potential microtubule targeting agents. The synthesis involved a Fisher indole cyclization of 2-amino-6-hydrazinylpyrimidin-4(3*H*)-one with cyclohexanone, followed by oxidation, chlorination and displacement with appropriate anilines. Compounds **6**, **14** and **15** had low nanomolar potency against MDA-MB-435 tumor cells and depolymerized microtubules. Compound **6** additionally had nanomolar GI_{50} values against 57 of the NCI 60-tumor panel cell lines. Mechanistic studies showed that **6** inhibited tubulin polymerization and [^{3}H]colchicine binding to tubulin. The most potent compounds were all effective in cells expressing P-glycoprotein or the βIII isotype of tubulin, which have been associated with clinical drug reisistence. Modeling studies provided the potential interactions of **6**, **14** and **15** within the colchicine site.

Introduction

Microtubules play a crucial role in normal cellular metabolism, in the orchestration of mitotic events and are validated targets for treating cancer.[2, 3] Microtubule-targeting compounds as antitumor agents have met with unprecedented clinical success and are

*To whom correspondence should be addressed. A.G., phone 412-396-6070, fax 412-396-5593, gangjee@duq.edu; S.L.M., phone 210-567-4788, fax 210-567-4300, mooberry@uthscsa.edu.
†These authors contributed equally to this work.

Supporting Material: Results from elemental analysis and High Resolution Mass Spectra (HRMS) (ESI). This material is available free of charge via the Internet.

frequently referred to as antimitotic agents. More recently, however, the idea that disruption of interphase events play a major role in the anticancer actions of microtubule targeting drugs has gained new attention.[4] Chemotherapeutic regimens often include a taxane or a vinca alkaloid (Figure 1). The taxanes, including paclitaxel, docetaxel and nab-paclitaxel, are utilized primarily for the management of adult solid tumors, including breast, ovarian, and prostate, as well as cancers of the head and neck and non-small cell lung cancer. The vinca alkaloids (vincristine, vinblastine, and vinorelbine) are most often used for hematological malignancies, such as lymphomas and leukemias. A simplistic classification of microtubule targeting agents includes microtubule stabilizers (taxanes) and microtubule destabilizers (vincas).[5] The taxanes bind at the taxane site located on β-tubulin in the interior surface of microtubules where they stabilize cellular microtubules while the vincas bind within the vinca domain of β-tubulin located on the outer surface of the microtubule and destabilize microtubules causing a net loss of cellular microtubules. Compounds that bind within another, non-overlapping binding site on tubulin, the colchicine site, elicit the same "destabilizing" effect as observed with the vincas.[6] Although colchicine, due to its high toxicity, is not used as an anticancer agent, colchicine-site binding drugs, such as combretastatin A-4 (CA-4), are advancing in clinical trials. CA-4P, the phosphorylated prodrug of CA-4, was recently evaluated in ovarian, non-small cell lung cancer and anaplastic thyroid cancer and additional studies are planned.[7] CA-1P is currently being evaluated in a Phase I trial in acute myelogenous leukemia (AML) and in myelodysplastic syndrome (MDS).[8]

Despite the exceptional success of microtubule targeting agents in cancer chemotherapy, multidrug resistance (MDR) is a major limitation in their clinical use. One of the mechanisms for tumor resistance is the inherent expression of MDR proteins like P-glycoprotein (Pgp), an ATP-binding cassette (ABC) transporter.[9] These transporters can act as drug efflux pumps and reduce the accumulation of Pgp substrates in tumor cells.[10] In addition to innate resistance, the administration of the taxanes and other Pgp substrates has been associated with acquired tumor resistance due to Pgp overexpression.[11] Attempts to reverse drug resistance by combining microtubule agents with inhibitors of drug efflux proteins have been disappointing.[12] The fact that microtubule-binding agents are substrates for ABC efflux pumps also limits their transport into the central nervous system (CNS) and represents an obstacle to their oral administration, suggesting that new compounds, which are less susceptible to transport by ABC proteins, could lead to improved efficacy in MDR tumors.[13]

Another mechanism for resistance to the taxanes and the vinca alkaloids is the expression of the βIII isotype of tubulin. In a variety of cell lines, overexpression of βIII-tubulin is associated with resistance to tubulin-binding antimitotic agents.[14, 15] Clinically, expression of βIII-tubulin in ovarian, breast and non-small cell lung cancers is linked with resistance to the taxanes or vinorelbine and with poor prognosis (reviewed in reference 3). Although many other tubulin-based mechanisms of multidrug resistance have been identified in cell lines, thus far, only expression of Pgp and the βIII tubulin isotype have been linked with clinical resistance to diverse tubulin binding agents.[16]

We[17] had previously reported *N*-(4-methoxyphenyl)-*N*,2-dimethyl-7*H*-pyrrolo[2,3-*d*]pyrimidin-4-amine **1** (Figure 2) as a microtubule-targeting agent with nanomolar potency (Table 1). We showed that **1** functions by a mechanism similar to that of colchicine and CA-4 and inhibits tumor cells with equal potency without regard to their expression of Pgp or βIII-tubulin. In addition, compound **1** inhibits the binding of [^{3}H]colchicine to tubulin, suggesting that it binds within the colchicine site. With **1** as the lead compound, we designed the tricyclic pyrimido[4,5-*b*]indole structure A (Figure 2), to develop inhibitors of tubulin similar to or more potent than **1**. The additional C-ring introduced in scaffold A

conformationally restricts the rotation of the aniline moiety and was hypothesized to be favorable for additional interactions within the colchicine site on tubulin. To ascertain the importance of various groups on the tricyclic scaffold to biological activity, compounds **2–15** were designed with variations at the 4-nitrogen and the aniline phenyl group. Compounds **2–5**, **8**, **9**, and **12** did not have a methylated aniline nitrogen. A methyl group at N4 was anticipated to further restrict rotation of the C4–N4 bond as well as the N4-C' bond to also restrict phenyl ring rotation. Activity of such analogs was anticipated to reflect conformational restriction as well as hydrophobic interactions of the N4-methyl moiety with the colchicine site on tubulin. Compounds **6**, **7**, **10**, **11**, **13**, and **15** represent such conformationally restricted analogs with a N4-methyl substitution akin to **1**. Compound **14** was designed with a larger ethyl group at the N4-position to determine the effect of size at the N4-position on biological activity. Molecular modeling (see below) does indeed predict that the N4-alkyl groups lie in the C5–C6 region of *N*-deacetyl-*N*-(2-mercaptoacetyl)colchicine (DAMA colchicine) when docked into tubulin.

To determine the importance of the nature and position of the aniline substituent on activity, compounds with electron donating 4'-OMe (**4**, **5**, **6**, **7**, **14**), 3'-OMe (**2**, **3**, **10**, **11**), 4'-Me (**13**), 4'-OEt (**15**) and electron withdrawing 3'-Br (**8**, **9**) substituents were designed. The 3', 4',5'-triOMePh group is present in colchicine and CA-4, thus it was of interest to study the effect of this group when combined with the pyrimido[4,5-*b*]indole scaffold in **12**. Molecular modeling (see below) also predicts that such a 3',4',5'-triOMePh analog could mimic colchicine.

The 2-CH_3 in **1** is isosterically replaced with a 2-NH_2 (**2**, **4**, **6, 8**, **10**, **12–15**). The 2-CH_3 and 2-NH_2 groups are oriented towards the solvent (see molecular modeling below, Figures 6, 7 and 8) and hence the 2-NH_2 should be more compatible and was the preferred choice in this study. The 2-NH_2 group was protected with a pivaloyl group in **3**, **5**, **7**, **9** and **11** as intermediates in the synthesis of **2**, **4**, **6**, **8** and **10**, respectively, and it was of interest to test these protected analogs as well to study the importance to biological activity of a free 2-NH_2 as compared with a 2-CH_3 and to determine whether additional binding ability was conferred by the pivaloyl group.

Chemistry

The synthesis of target compounds commenced from commercially available 2-amino-6-chloropyrimidin-4(3*H*)-one **16** (Scheme 1) using a reported method[18] to obtain **17** in 46% yield. A thermal Fisher indole cyclization of **17** and cyclohexanone in diphenyl ether furnished the tricyclic scaffold **18**. The partially saturated ring in **18** was oxidized using 10% Pd/C to provide **19** in 57% yield. Pivaloyl protection of **19** gave **20**, and subsequent chlorination afforded the common intermediate **21**. Compound **21** was treated with various substituted anilines **22–26** in isopropanol and a catalytic amount (1–3 drops) of conc. HCl at reflux to provide **3**, **5**, **7**, **9**, and **11**, respectively in 37–80% yield. The pivaloyl group in **3**, **5**, **7**, **9**, and **11** was removed by basic hydrolysis of the 2-amide linkage in these compounds using 1 N NaOH to give compounds **2**, **4**, **6**, **8**, and **10**, respectively, in yields ranging from 53 to 93%. To address the water solubility problems associated with paclitaxel and other antimitotic agents, the water soluble HCl salt of **6** (**6**·HCl) was obtained by bubbling anhydrous HCl gas through a solution of **6** (55 mg) in diethyl ether, ethyl acetate and chloroform.

Reaction of **21** with appropriate anilines **27–29** (Scheme 2) and catalytic conc. HCl (1–3 drops) in *n*-butanol at reflux provided **12–14**, respectively, in 31–79% yield. Compound **21** upon treatment with **30** in isopropanol afforded target compound **15** in 71% yield.

Compounds **29**[19] and **30**[20] were synthesized from **31** and **32**, respectively, using reported procedures.

Biological Evaluations

Compounds **2–15** were designed as microtubule targeting agents, and they were first tested for their ability to disrupt cellular microtubules (Table 1). Compounds **2–5** and **7–13** had no effects on cellular microtubules at concentrations as high as 10 or 40 μM. It should be noted that all the N4-desalkyl analogs including **4** (4'-OMe) and **12** (3',4',5'-triOMe) were inactive. Among the 2-amino- N4-alkyl analogs, the 4'-O-alkyl analogs **6**, **14** and **15** were active whereas the analogs **13** (4'-Me) and **10** (3'-OMe) were inactive. The inactivity of **13** can be attributed to the lack of hydrogen bonding ability that is observed with the higly active **6** (Figure 6), which had an EC_{50}, the concentration required to cause 50% loss of cellular microtubules, of 105 nM (Table 1). The pivaloyl protected analog of **6**, compound **7**, is inactive indicating the intolerance of pivaloyl group in the binding site. The data indicates that N4-alkyl, 4'-O-alkyl and a free 2-NH_2 group are important for activity. Compound **6** was 55-times more potent than **1** in depolymerizing cellular microtubules and 8-times less potent than CA-4 for this effect. The antiproliferative effects of **6** were evaluated against the drug sensitive MDA-MB-435 cell line using the sulforhodamine B assay.[21, 22] The data (Table 1) indicated that **6** had potent antiproliferative effects with an IC_{50}, the concentration required to cause 50% inhibition of proliferation, of 14.7 nM. Compound **6** was 12-fold more potent than **1** for inhibition of proliferation, indicating that the addition of the C-ring and isosteric replacement of the 2-CH_3 with 2-NH_2 was favorable. The EC_{50}/IC_{50} ratio gives an indication of the linkage of the microtubule depolymerizing effects and the antiproliferative activities. Compound **6** had a substantially lower EC_{50}/IC_{50} ratio of 7.1 as compared with **1**, which had a ratio of 31.7. The high ratio obtained with **1** suggests that additional mechanisms are implicated in the ability of this compound to inhibit cell proliferation. A low ratio provides an indication of a tighter linkage of the microtubule depolymerizing effects and inhibition of cell proliferation. The ratio for CA-4, at 3.8, was even lower than that of compound **6**, suggesting the possibility that **6** might impact microtubule-independent mechanisms of growth inhibition.

Two additional microtubule active compounds **14** and **15** were identified in this series. They were also potent microtubule depolymerizers with EC_{50} values of 198 and 83 nM, respectively (Table 1). These compounds were potent inhibitors of tumor cell proliferation with IC_{50} values of 23.5 and 14.4 nM against MDA-MB-435 melanoma cells, respectively. Consistent with the activities of **6**, compounds **14** and **15** had EC_{50}/IC_{50} ratios of 8.4 and 6.5, again suggesting a much closer linkage of the microtubule depolymerizing effects and antiproliferative activities than were observed with **1**.

In the preclinical National Cancer Institute 60 cancer cell line panel, compound **6** exhibited potent GI_{50}s (Table 2).[24]

The microtubule disrupting effects of **6** are shown in Figure 3 in a cell-based immunofluorescence assay. Compound **6** caused extensive loss of the interphase microtubule network, similar to the effects of CA-4. Similar effects were noted for **14** and **15** (data not shown).

Consistent with its ability to disrupt interphase microtubules (Figure 3), compounds **6**, **14** and **15** caused the formation of aberrant mitotic spindles (data not shown). The effects of **6** on cell cycle distribution were evaluated by flow cytometry (Figure 4), which showed accumulation of cells in the G_2/M phase of the cell cycle.

The ability of **6**, **14** and **15** to circumvent Pgp-mediated drug resistance was evaluated by using an SK-OV-3 isogenic cell line pair (Table 3). This cell line pair consists of the parental SK-OV-3 ovarian carcinoma cell and a subline, the SK-OV-3 MDR-1-6/6, which was generated by transduction of *MDR-1* gene and clonal isolation.[23] The ability of compounds to overcome Pgp-mediated drug resistance was evaluated by examining the sensitivity of the two cell lines to the compounds. The IC_{50} values obtained in the Pgp-expressing MDR-1-6/6 cells were divided by the IC_{50} obtained in the parental cells to generate a relative resistance value, designated Rr. A low Rr indicates that the cell lines have similar sensitivity to the compound and that the compound is able to overcome the expression of Pgp and suggests that it is a poor substrate for transport by Pgp. A high Rr value is found with known Pgp substrates, including paclitaxel. In this cell line pair, the relative resistance (Rr) value of paclitaxel was 590 while the Rr value of **6** was 1.2, comparable with the Rr value obtained with CA-4 of 1.2. Similar results were obtained with **14** and **15** with Rr values of 1.4 and 1.3 respectively (Table 3). Thus, compounds **6**, **14** and **15** are effective in this cell line that overexpresses Pgp and the data suggests that these compounds are poor substrates for transport by Pgp and thus have advantages over paclitaxel and the vincas. A second mechanism of drug resistance that is associated with treatment failure with tubulin binding agents is the expression of βIII-tubulin. A HeLa cell line pair was used to study the effects of βIII-tubulin on the potency of **6**, **14** and **15** (Table 3). The WT βIII cell line was generated from HeLa cells transfected with the gene for βIII-tubulin.[23] The IC_{50} of each of these compounds were determined in the two cell lines and then the relative resistance (Rr) value was calculated by dividing the IC_{50} of the βIII expressing cell line by the IC_{50} value obtained in the HeLa parental cell line. Compound **6** has an Rr value of 1.0, compound **14** a Rr of 1.4 and compound **15** a Rr of 0.8 in this cell line pair, suggesting that they overcome drug resistance mediated by βIII-tubulin as compared with paclitaxel, which has a Rr of 5.8 in these cell lines. Thus, compounds **6**, **14** and **15** potently inhibited the proliferation of human cancer cells without regard to their expression of Pgp or βIII-tubulin.

Studies were conducted to determine if **6**, **14** and **15** inhibited the polymerization of purified bovine brain tubulin,[25, 26] as would be predicted from the effects in cells. These biochemical studies provided an indication of a direct interaction of the compounds with tubulin. An initial study shown in Figure 5 indicated that **6** was a potent inhibitor of tubulin assembly. Compounds **6**, **14** and **15** were therefore compared with CA-4 as inhibitors of tubulin assembly in a quantitative study (Table 4). In this assay, compounds **6**, **14** and **15** inhibited tubulin assembly about as well as CA-4. The data in Table 4 also shows that these compounds bind to the colchicine site on tubulin, since they inhibited [^{3}H]colchicine binding to the protein. The potency of this inhibition with **6**, **14** and **15** was better than with **1** although somewhat less than the inhibition obtained with CA-4.

Molecular Modeling

In an attempt to explain the potent activity of **6** against tubulin, we performed molecular modeling studies in the colchicine binding site of tubulin (PDB: 1SA0),[28] using MOE 2008.10[29] and methods reported previously in the docking studies of **1**.[17] Multiple low energy binding poses (within 1 kcal/mol of the lowest energy) were observed for **6** and can be accounted for by the large volume of the colchicine binding site.[28, 30] The docked pose of **6** (Figure 6) had a score of −7.6342 kcal/mol compared to the docked pose of **1**,[17] which had a score of −6.0330 kcal/mol. Comparison of the docked conformation of **6** with the crystal structure conformation of DAMA colchicine showed an overlap of the 4'-OCH_3 phenyl group of **6** with the trimethoxybenzene A-ring of DAMA colchicine, with the 4'-OCH_3 moiety overlapping the 2'-OCH_3 of DAMA colchicine. This conformation aids the formation of a hydrogen bond between Cysβ241 of tubulin and the oxygen atom of the 4'-

OCH_3 of **6** (residue number follows the modeling convention used by Ravelli et al.[28] rather than the actual residue numbers in the beta tubulin sequence). The phenyl ring interacts with Cysβ241, Leuβ248, Alaβ250, Leuβ255, Alaβ316 and Valβ318. The importance of the *N*-CH_3 group of **6** is that it mimics the C5–C6 atoms of the B-ring of DAMA colchicine and interacts with Leuβ248, Alaβ250, Lysβ254, and Leuβ255. Additionally, the *N*-CH_3 group aids in maintaining the relative conformation of the pyrimido[4,5-*b*]indole and the phenyl ring. The pyrimido[4,5-*b*]indole scaffold of **6** overlaps with the C-ring of DAMA colchicine and is stabilized by hydrophobic interactions with Alaα180, Valα181, Leuβ248, Leuβ255, Metβ259, and Alaβ316. The indole NH forms a hydrogen bond with the backbone carbonyl of Thrα179 and mimics the hydrogen bond formed between the C9-carbonyl of DAMA colchicine and the backbone NH of Thrα179. The 2-NH_2 moiety of **6** is exposed towards the solvent front and was not found to interact with the amino acids of the active site of tubulin. The inactivity of the pivaloyl protected **6**, compound **7**, can also be explained by the exposure of the hydrophobic pivaloyl moiety of **7** to the solvent. Comparison of the docked conformations of **1** and **6** indicates that the larger tricyclic scaffold of **6** better fits the large binding pocket of the colchicine site in the DAMA colchicine X-ray crystal structure as compared to the bicyclic scaffold of **1**. In addition, the pyrimido[4,5-*b*]indole scaffold of **6** not only retains the binding interactions of the pyrrolo[2,3-*d*]pyrimidine scaffold of **1** but also provides additional hydrophobic interactions with the pocket residues which accounts, in part, for the improved docking score of **6** compared to **1** in tubulin (Figure 6).

Comparison of the docked poses of **14** (Figure 7) and **6** (Figure 6) shows that the presence of the N-Et group causes a shift in the bound conformation of the 4'-OMe-phenyl groups of the two molecules. This change in the bound conformation of the 4'-OMe-phenyl group of **14** still retains the binding interactions of the corresponding 4'-OMe-phenyl group of **6** and can be explained by the large volume of the binding pocket. The N-Et group of **14** forms hydrophobic interactions with Leuβ248, Alaβ250, Leuβ252, Leuβ255 and the carbon atoms of the side chain of Lysβ254. The docking score of **14** was −7.6817 kcal/mol, comparable to that of **6** (−7.6342 kcal/mol) and **14** and **6** have similar activities.

The docked pose of **15** (Fig. 8) retains binding interactions seen in the docked pose of **6** (Fig. 6) in the tubulin active site. The 4'-OEt substitution of **15** forms hydrophobic interactions with Valα318, Ileβ378, Cysβ241 and Leuβ242 in the binding pocket. Comparison of the docked poses of **6** and **15** indicates that the shorter 4'-OMe substitution of **6** does not interact with Ileβ378. This additional hydrophobic interaction could account, in part, for the improved activity of **15** compared to **6** and is also reflected in the slight improvement in the docking score of **15** (−7.7512 kcal/mol) compared to **6** (−7.6342 kcal/mol).

In conclusion, we report the synthesis and identification of novel antimitotic agents containing the pyrimido[4,5-*b*]indole scaffold, albeit with stringent substitution requirements. Tricyclic compound **6** was several fold more potent against tumor cells in culture than bicyclic **1**, indicating that bulk in the form of the C-ring and isosteric replacement of the 2-CH_3 with 2-NH_2 is favored. The presence of a N4-CH_3 and 4'-OCH_3 (**6**) is important for activity while a N4-C_2H_5 (**14**) or a 4'-OC_2H_5 (**15**) maintains activity. This study also provided an explanation of the importance of the *N*-CH_3 moiety of **6** for biological activity via molecular modeling. Compound **6** is currently undergoing hollow fiber assay at the National Cancer Institute, National Institutes of Health. Compound **6**·HCl is freely soluble in water and indicates water-soluble version of potent antitubulin agent **6**. It is anticipated that this should circumvent the water solublitiy problems associated with paclitaxel and other antimitotic agents. Hence, compound **6** serves as an important lead compound for the development of further compounds for preclinical evaluations as

antimitotic agents that circumvent some of the major drawbacks of paclitaxel, such as tumor resistance and lack of water solubility.

Experimental

Analytical samples were dried in vacuo (0.2 mm Hg) in a CHEM-DRY drying apparatus over P_2O_5 at 50 °C. Melting points were determined on a digital MEL-TEMP II melting point apparatus with FLUKE 51 K/J electronic thermometer and are uncorrected. Nuclear magnetic resonance spectra for proton (^{1}H NMR) were recorded on Bruker Avance II 400 (400 MHz) and 500 (500 MHz) NMR systems. The chemical shift values are expressed in ppm (parts per million) relative to tetramethylsilane as an internal standard: s, singlet; d, doublet; t, triplet; q, quartet; m, multiplet; br, broad singlet. Thin-layer chromatography (TLC) was performed on Whatman Sil G/UV254 silica gel plates with a fluorescent indicator, and the spots were visualized under 254 and 366 nm illumination. Proportions of solvents used for TLC are by volume. Column chromatography was performed on a 230−400 mesh silica gel (Fisher Scientific) column. Elemental analyses were performed by Atlantic Microlab, Inc., Norcross, GA. Elemental compositions are within ±0.4% of the calculated values and indicate > 95% purity. Fractional moles of water or organic solvents frequently found in some analytical samples could not be prevented despite 24−48 h of drying in vacuo and were confirmed where possible by their presence in the ^{1}H NMR spectra. Mass spectrum data were acquired on an Agilent G6220AA TOF LC/MS system using the nano ESI (Agilent chip tube system with infusion chip). All solvents and chemicals were purchased from Sigma-Aldrich Co. or Fisher Scientific Inc. and were used as received.

2-Amino-6-hydrazinopyrimidin-4(3*H*)-one (17)

To a stirred suspension of 15.0 g (103 mmol) of **16** in 250 mL water was added 12 g (375 mmol) of anhydrous hydrazine, and the mixture was heated to reflux for 3 h. The resulting clear solution was cooled, and the precipitate that separated was collected by filtration, washed with water followed by ethanol and dried to give 6.6 g (46%) of **17** as a white solid. mp decomposes at 313 °C (Literature mp 314–315 °C).[31]

2-Amino-3,5,6,7,8,9-hexahydro-4*H*-pyrimido[4,5-*b*]indol-4-one (18)

A mixture of 2-amino-6-hydrazinopyrimidin-4(3*H*)-one **17** (350 mg, 2.5 mmol) and cyclohexanone (245 mg, 2.5 mmol) in diphenyl ether (30 ml) was stirred and heated at 120–130 °C in an oil bath overnight and then under reflux at 250 °C for 3 h. After cooling to room temperature, hexane (50 mL) was added, and the precipitated solid was collected by filtration. The solid was dried over P_2O_5, dissolved in methanol, and silica gel (three times the weight of solid) was added, following which the solvent was removed under reduced pressure to obtain a dry plug. The plug was loaded on top of a column packed with silica in chloroform. The weight of silica in the column was thirty times the weight of the plug. Flash chromatography using 20% methanol in chloroform afforded **18** (82%) as a yellow solid. TLC R_f 0.35 (chloroform-methanol 5:1); mp decomposes at 338 °C; ^{1}H NMR (DMSO-d^6) δ 1.64–1.69 (m, 4 H, 6-CH_2, 7-CH_2), 2.42 (m, 2 H, 5-CH_2), 2.53 (m, 2 H, 8-CH_2), 5.88 (s, 2 H, 2-NH_2, exch), 10.02 (s, 1 H, 3-NH, exch), 10.50 (s, 1 H, 9-NH, exch). Anal. calcd. for $C_{10}H_{12}N_4O$. 0.4 H_2O: C, 56.80; H, 6.10; N, 26.50; Found: C, 56.90; H, 6.06; N, 26.49.

2-Amino-3,9-dihydro-4*H*-pyrimido[4,5-*b*]indol-4-one (19)

A mixture of **18** (50 mg, 0.24) and 10% Pd/C (24 mg) in Ph_2O (5 mL) was heated to reflux for 3 h. The reaction mixture was cooled to room temperature, and DMF (20 mL) was added to dissolve the product. The catalyst was removed by filtration through celite and washed with DMF to give a solution that was evaporated to yield a solid residue. Hexane (25 mL)

was added to the residue, and the solid was filtered. The solid was dissolved in DMF (5 mL), and silica gel (1 g) was added. Solvent was removed under reduced pressure to afford a plug, which was loaded on top of a silica gel column in chloroform (the silica was thirty times the weight of the plug). The column was eluted with 20% methanol in chloroform to afford 28 mg of **19** as a pale white solid in 57% yield. TLC R_f 0.32 (chloroform-methanol 5:1); mp > 340 °C; ^{1}H NMR (DMSO-d^6) δ 6.51 (s, 2 H, NH_2), 7.03–7.10 (m, 2 H, Ar), 7.22–7.25 (m, 1 H, Ar), 7.68–7.70 (m, 1 H, Ar), 10.47 (s, 1 H, 3-NH, exch), 11.35 (s, 1 H, 9-NH, exch). HRMS (ESI) calcd. for $C_{10}H_8N_4O$: 200.0698, found: 200.0693.

2,2-Dimethyl-*N*-(4-oxo-4,9-dihydro-3*H*-pyrimido[4,5-*b*]indol-2-yl)propanamide (20)

Compound **19** (50 mg, 0.25 mmol), trimethyl acetic anhydride (6 g, 32 mmol), DMAP (16 mg, 0.13 mmol), and triethylamine (101 mg, 1 mmol) were dissolved in 8 mL of DMF. The mixture was heated at 60 °C for 40 h. The DMF and trimethyl acetic anhydride were removed under reduced pressure using an oil pump. The residue thus obtained was dissolved in methanol, and 3 g of silica gel was added to the solution. The solvent was removed under reduced pressure to afford a dry plug. The plug was loaded on top of a silica gel column in chloroform (the silica was twenty times the weight of the plug), which was eluted with 1% methanol in chloroform to afford 52 mg of **20** as a yellow solid in 73% yield. TLC R_f 0.67 (chloroform-methanol 5:1); mp decomposes at 322 °C; ^{1}H NMR (DMSO-d^6) δ 1.26 (s, 9 H, $C(CH_3)_3$), 7.17–7.21 (m, 1 H, Ar), 7.24–7.28 (m, 1 H, Ar), 7.43–7.45 (m, 1 H, Ar), 7.86–7.88 (m, 1 H, Ar), 11.12 (s, 1 H, NH, exch), 11.85 (s, 1 H, NH, exch), 12.03 (s, 1 H, NH, exch). Anal. calcd. for $C_{15}H_{16}N_4O_2$. 0.3 H_2O: C, 62.18; H, 5.77; N, 19.33; Found: C, 62.24; H, 5.83; N, 18.98.

N-(4-Chloro-9*H*-pyrimido[4,5-*b*]indol-2-yl)-2,2-dimethylpropanamide (21)

In a 50 mL round bottom flask was placed **20** (56 mg, 0.17 mmol) and phosphoryl trichloride (15 mL). The mixture was stirred and heated at reflux for 4 h. The phosphoryl trichloride was removed by evaporation under reduced pressure using a vacuum aspirator. The resulting residue was cooled in an ice and water mixture and neutralized with ammonium hydroxide solution to yield a precipitate that was filtered and dried over P_2O_5. The filtrate was extracted with chloroform and dried over sodium sulfate. The dry precipitate and filtrate were combined and dried under vacuum to provide 35 mg of **21** as a brown solid in 59% yield. TLC R_f 0.65 (chloroform-methanol 10:1); mp 234 °C; ^{1}H NMR (DMSO-d^6) δ 1.24 (s, 9 H, $C(CH_3)_3$), 7.34–7.38 (m, 1 H, Ar), 7.53–7.55 (m, 2 H, Ar), 8.15–8.17 (m, 1 H, Ar), 10.25 (s, 1 H, 2-NH, exch), 12.55 (s, 1 H, 9-NH, exch). Anal. calcd. for $C_{15}H_{15}ClN_4O$. 0.15 H_2O: C, 58.98; H, 5.04; N, 18.34; Cl, 11.60; Found: C, 59.00; H, 5.09; N, 17.97; Cl, 11.83.

General procedure for the synthesis of 3, 5, 7, 9, and 11

Compound **21** (1 equivalent) was dissolved in isopropanol, and to this solution was added a substituted aniline (7.5 equivalents). Three drops of conc. HCl were added, and the resulting mixture was stirred and heated to reflux for 18–120 h, depending upon the aniline used. For work up of this reaction mixture, the solvent was removed under reduced pressure, the mixture was basified with ammonia in methanol, dissolved in methanol, and silica gel was added, and the solvent was removed by evaporation to yield a dry plug. The plug was loaded on top of a silica gel column in chloroform (the silica was fifty times the weight of the plug), and the column was eluted with 0.2% methanol in chloroform to obtain compounds **3**, **5**, **7**, **9**, and **11** in yields of 37–80%.

***N*-{4-[(3-Methoxyphenyl)amino]-9*H*-pyrimido[4,5-*b*]indol-2-yl}-2,2-dimethylpropanamide (3)—**Using the general procedure described above, the reaction of

21 (160 mg, 0.52 mmol) and 3-methoxyaniline **22** (488 mg, 3.96 mmol) was run for 36 h, to provide 107 mg of **3** as an off white solid in 52% yield. TLC R_f 0.64 (chloroform-methanol 15:1); mp 219.4–220.2 °C; ^{1}H NMR (DMSO-d^6) δ 1.23 (s, 9 H, $C(CH_3)_3$), 3.81 (s, 3 H, OCH_3), 6.57–6.59 (m, 1 H, Ar), 7.17–7.26 (m, 2 H, Ar), 7.36–7.38 (m, 1 H, Ar), 7.45–7.47 (m, 1 H, Ar), 7.51–7.53 (m, 1 H, Ar), 7.9 (s, 1 H, Ar), 8.29–8.31 (m, 1 H, Ar), 8.62 (s, 1 H, 4-NH, exch), 9.59 (s, 1 H, 2-NH, exch), 11.85 (s, 1 H, 9-NH, exch). Anal. calcd. for $C_{22}H_{23}N_5O_2$. 0.45 CH_3OH: C, 66.76; H, 6.19; N, 17.34; found: C, 66.95; H, 6.18; N, 16.96.

***N*-{4-[(4-Methoxyphenyl)amino]-9*H*-pyrimido[4,5-*b*]indol-2-yl}-2,2-dimethylpropanamide (5)—**Using the general procedure described above, the reaction of **21** (80 mg, 0.26 mmol) and 4-methoxyaniline **23** (244 mg, 1.98 mmol) was run for 18 h, to provide 52 mg of **5** as a white solid in 51% yield. TLC R_f 0.55 (chloroform-methanol 15:1); mp 266.8–267 °C; ^{1}H NMR (DMSO-d^6) δ 1.23 (s, 9 H, $C(CH_3)_3$), 3.75 (s, 3 H, OCH_3), 6.88–6.90 (d, 2 H, Ar), 7.19–7.22 (m, 1 H, Ar), 7.31–7.35 (m, 1 H, Ar), 7.43–7.44 (m, 1 H, Ar), 7.90–7.93 (d, 2 H, Ar), 8.26–8.28 (m, 1 H, Ar), 8.55 (s, 1 H, 4-NH, exch), 9.41 (s, 1 H, 2-NH, exch), 11.79 (s, 1 H, 9-NH, exch). Anal. calcd. for $C_{22}H_{23}N_5O_2$. 0.4 H_2O: C, 66.62; H, 6.04; N, 17.65; Found: C, 66.61; H, 6.00; N, 17.37.

***N*-{4-[(4-Methoxyphenyl)(methyl)amino]-9*H*-pyrimido[4,5-*b*]indol-2-yl}-2,2-dimethylpropanamide (7)—**Using the general procedure described above, the reaction of **21** (180 mg, 0.59 mmol) and 4-methoxy-*N*-methylaniline **24** (612 mg, 4.46 mmol) was run for 72 h, to provide 109 mg of **7** as brown crystals in 45% yield. TLC R_f 0.62 (chloroform-methanol 15:1); mp 248.2–249 °C; ^{1}H NMR (DMSO-d^6) δ 1.27 (s, 9 H, $C(CH_3)_3$), 3.63 (s, 3 H, OCH_3), 3.75 (s, 3 H, NCH_3), 5.78–5.80 (m, 1 H, Ar), 6.64–6.67 (m, 1 H, Ar), 6.93–6.95 (m, 2 H, Ar), 7.11–7.15 (m, 1 H, Ar), 7.22–7.31 (m, 3 H, Ar), 9.52 (s, 1 H, 2-NH, exch), 11.83 (s, 1 H, 9-NH, exch). Anal. calcd. for $C_{23}H_{25}N_5O_2$. 0.55 CH_3OH: C, 67.16; H, 6.51; N, 16.63. Found: C, 67.33; H, 6.49; N, 16.28. HRMS (ESI) calcd. for $C_{23}H_{25}N_5O_2$: 403.2008, found: 403.1988.

***N*-{4-[(3-Bromophenyl)amino]-9*H*-pyrimido[4,5-*b*]indol-2-yl}-2,2-dimethylpropanamide (9)—**Using the general procedure described above, the reaction of **21** (181 mg, 0.59 mmol) and 3-bromoaniline **25** (771 mg, 4.48 mmol), was run for 26 h, to provide 209 mg of **9** as a white solid in 80% yield. TLC R_f 0.28 (chloroform-methanol 20:1); mp 286.7–287.5 °C; ^{1}H NMR (DMSO-d^6) δ 1.27 (s, 9 H, $C(CH_3)_3$), 7.19–7.21 (m, 1 H, Ar), 7.25–7.29 (m, 2 H, Ar), 7.37–7.40 (m, 1 H, Ar), 7.48–7.49 (m, 1 H, Ar), 8.18–8.20 (m, 1 H, Ar), 8.37–8.39 (m, 1 H, Ar), 8.45–8.46 (m, 1 H, Ar), 8.79 (s, 1 H, 4-NH, exch), 9.64 (s, 1 H, 2-NH, exch), 11.89 (s, 1 H, 9-NH, exch). Anal. calcd. for $C_{21}H_{20}BrN_5O$: C, 57.54; H, 4.59; N, 15.97; Br, 18.22; Found: C, 57.34; H, 4.65; N, 15.80; Br, 17.96.

***N*-{4-[(3-Methoxyphenyl)(methyl)amino]-9*H*-pyrimido[4,5-*b*]indol-2-yl}-2,2-dimethylpropanamide (11)—**Using the general procedure described above, the reaction of **21** (180 mg, 0.59 mmol) and 3-methoxy-*N*-methylaniline **26** (612 mg, 4.46 mmol) was run for 120 h, to provide 88 mg of **11** as a brown solid in 37% yield. TLC R_f 0.57 (chloroform-methanol 15:1); mp 288.5–289.4 °C; ^{1}H NMR (DMSO-d^6) δ 1.27 (s, 9 H, $C(CH_3)_3$,) 3.62 (s, 3 H, OCH_3), 3.71 (s, 3 H, NCH_3), 5.89–5.91 (m, 1 H, Ar), 6.68–6.81 (m, 2 H, Ar), 6.96–7.34 (m, 5 H, Ar), 9.60 (s, 1 H, 2-NH, exch), 11.89 (s, 1 H, 9-NH, exch). HRMS (ESI) calcd. for $C_{23}H_{25}N_5O_2$ $(M+H)^+$: 404.2087, found: 404.2080.

General procedure for the synthesis of 2, 4, 6, 8, and 10

Compounds **3**, **5**, **7**, **9**, and **11** were dissolved individually in isopropanol. About 4 mL of 1 N NaOH was added to this solution, and the resulting mixture was stirred and heated to reflux for 14 h. For work up of this reaction mixture, the solvent was removed under

reduced pressure, and the residue was dried over P_2O_5. The dry residue was dissolved in methanol, and silica gel was added. The solvent was removed by evaporation to yield a dry plug. The plug was loaded on top of a silica gel column in chloroform (the weight of the silica was 15 times that of the plug), and the column was eluted with 1% methanol in chloroform to yield compound **2**, **4**, **6**, **8**, or **10**. These compounds were washed with nonpolar solvents (hexane, diethyl ether) and dried in vacuo. The yields ranged from 53 to 93%.

***N*^{4}-(3-Methoxyphenyl)-9*H*-pyrimido[4,5-*b*]indole-2,4-diamine (2)—**Using the general procedure described above, the reaction of **3** (80 mg, 0.20 mmol) and 1 N NaOH provided 40 mg of **2** as an off-white solid in 64% yield. TLC R_f 0.30 (chloroform-methanol 15:1); mp 208.9–209.1 °C; ^{1}H NMR (DMSO-*d6*) δ 3.76 (s, 3 H, OCH_3), 6.19 (s, 2 H, NH_2, exch), 7.09–7.17 (m, 1 H, Ar), 7.18–7.21 (m, 1 H, Ar), 7.28–7.29 (m, 2 H, Ar), 7.41–7.42 (m, 1 H, Ar), 7.48–7.49 (m, 2 H, Ar), 8.03–8.05 (m, 1 H, Ar), 8.26 (s, 1 H, 4-NH, exch), 11.27 (s, 1 H, 9-NH, exch). Anal. calcd. for $C_{17}H_{15}N_5O$. 0.35 CH_3OH: C, 65.83; H, 5.22; N, 22.12. Found: C, 66.08; H, 5.22; N, 21.81.

***N*^{4}-(4-Methoxyphenyl)-9*H*-pyrimido[4,5-*b*]indole-2,4-diamine (4)—**Using the general procedure described above, the reaction of **5** (90 mg, 0.23 mmol) and 1 N NaOH provided 65 mg of **4** as a transparent solid in 92% yield. TLC R_f 0.34 (chloroform-methanol 15:1); mp 225.2–225.6 °C; ^{1}H NMR (DMSO-*d*^{6}) δ 3.74 (s, 3 H, OCH_3), 6.05 (br, 2 H, NH_2, exch), 6.88–6.90 (d, 2 H, Ar), 7.05–7.09 (m, 1 H, Ar), 7.13–7.17 (m, 1 H, Ar), 7.26–7.28 (m, 1 H, Ar), 7.62–7.64 (d, 2 H, Ar), 8.05–8.07 (m, 1 H, Ar), 8.16 (s, 1 H, 4-NH, exch), 11.20 (s, 1 H, 9-NH, exch). Anal. calcd. for $C_{17}H_{15}N_5O$. 0.15 $(C_2H_5)_2O$: C, 66.79; H, 5.25; N, 22.13. Found: C, 66.77; H, 5.08; N, 22.13.

***N*^{4}-(4-Methoxyphenyl)-*N*^{4}-methyl-9*H*-pyrimido[4,5-*b*]indole-2,4-diamine (6)—**Using the general procedure described above, the reaction of **7** (90 mg, 0.22 mmol) and 1 N NaOH provided 66 mg of **6** as a white solid in 93% yield. TLC R_f 0.27 (chloroform-methanol 15:1); mp 245.3–245.7 °C; ^{1}H NMR (DMSO-*d*^{6}) δ 3.48 (s, 3 H, OCH_3), 3.71 (s, 3 H, NCH_3), 5.75–5.77 (m, 1 H, Ar), 6.20 (s, 2 H, NH_2, exch), 6.51–6.55 (m, 1 H, Ar), 6.87–6.90 (m, 1 H, Ar), 6.95–6.97 (m, 1 H, Ar), 7.12–7.15 (m, 4 H, Ar), 11.22 (s, 1 H, 9-NH, exch). Anal. calcd. for $C_{18}H_{17}N_5O$. 0.17 H_2O: C, 67.05; H, 5.42; N, 21.72; Found: C, 67.06; H, 5.37; N, 21.56.

***N*^{4}-(3-Bromophenyl)-9*H*-pyrimido[4,5-*b*]indole-2,4-diamine (8)—**Using the general procedure described above, the reaction of **9** (209 mg, 0.47 mmol) and 1 N NaOH provided 128 mg of **8** as a white solid in 76% yield. TLC R_f 0.36 (chloroform-methanol 15:1); mp 233.6 °C; ^{1}H NMR (DMSO-*d*^{6}) δ 6.26 (br, 2 H, NH_2, exch), 7.09–7.13 (m, 1 H, Ar), 7.15–7.20 (m, 2 H, Ar), 7.23–7.25 (m, 1 H, Ar), 7.28–7.30 (m, 1 H, Ar), 7.94–7.96 (m, 1 H, Ar), 8.01–8.02 (m, 1 H, Ar), 8.08–8.09 (m, 1 H, Ar), 8.44 (s, 1 H, 4-NH, exch), 11.32 (s, 1 H, 9-NH, exch). Anal. calcd. for $C_{16}H_{12}BrN_5$: C, 54.25; H, 3.41; N, 19.77; Br, 22.55; Found: C, 54.38; H, 3.48; N, 19.56; Br, 22.29.

***N*^{4}-(3-Methoxyphenyl)-*N*^{4}-methyl-9*H*-pyrimido[4,5-*b*]indole-2,4-diamine (10)—**Using the general procedure described above, the reaction of **11** (100 mg, 0.24 mmol) and 1 N NaOH provided 58 mg of **10** as a white solid in 53% yield. TLC R_f 0.34 (chloroform-methanol 15:1); mp 233.6 °C; ^{1}H NMR (DMSO-*d*^{6}) δ 3.55 (s, 3 H, OCH_3), 3.58 (s, 3 H, NCH_3), 5.87–5.89 (m, 1 H, Ar), 6.17–6.18 (m, 1 H, Ar), 6.27 (br, 2 H, NH_2, exch), 6.55–6.59 (m, 1 H, Ar), 6.67–6.74 (m, 2 H, Ar), 6.96–7.03 (m, 1 H, Ar), 7.14–7.22 (m, 1 H, Ar), 11.27 (s, 1 H, 9-NH, exch). HRMS (ESI) calcd. for $C_{18}H_{17}N_5O$ $(M+H)^+$: 320.1503, found: 320.1511.

4-((4-Methoxyphenyl)(methyl)amino)-9*H*-pyrimido[4,5-*b*]indol-2-aminium chloride (6·HCl)—Compound **6** (55 mg) was dissolved in chloroform (0.5 mL), ethyl acetate (2 mL) and anhydrous ether (20 mL), and then HCl gas was bubbled into the solution till precipitation ceased. The white solid was collected by filtration and dried over P_2O_5 to afford **6**·HCl in 70% yield. TLC R_f 0.27 (chloroform-methanol 15:1 and 4 drops of NH_4OH); mp >250 °C; ^{1}H NMR (DMSO-d^6) δ 3.66 (s, 3 H, OCH_3), 3.79 (s, 3 H, NCH_3), 5.50–5.52 (m, 1 H, Ar), 6.65–6.69 (m, 1 H, Ar), 7.00–7.02 (m, 2 H, Ar), 7.10–7.13 (m, 1 H, Ar), 7.33–7.35 (m, 1 H, Ar), 7.41–7.43 (m, 2 H, Ar), 7.74 (br, 3 H, NH_3^+, exch), 12.36 (s, 1 H, 9-NH, exch). Anal. calcd. for $C_{18}H_{18}ClN_5O$: C, 60.76; H, 5.10; N, 19.68; Cl, 9.96; Found: C, 60.55; H, 5.14; N, 19.41; Cl, 9.75.

General procedure for the synthesis of 12–14

To a round bottom flask were added **21**, appropriate substituted aniline, 1–3 drops of concentrated HCl and 50 mL of *n*-butanol. The reaction mixture was heated under reflux. After cooling to rt, *n*-butanol was removed under reduced pressure, and purification was performed by column chromatography using 1% methanol in chloroform as the eluant.

***N*^{4}-(3,4,5-Trimethoxyphenyl)-9*H*-pyrimido[4,5-*b*]indole-2,4-diamine (12)—**Using the general procedure described above, the reaction of **21** (100 mg, 0.33 mmol) with 3,4,5-trimethoxyaniline **27** (302 mg, 1.65 mmol) and 3 drops of conc. HCl for 6 h afforded **12** in 79% yield. TLC R_f 0.13 (chloroform-methanol 15:1 with 2 drops concentrated NH_4OH); mp 248–248.7 °C; ^{1}H NMR (DMSO-d^6) δ 3.64 (s, 3 H, 4-OCH_3), 3.80 (s, 6 H, 3-OCH_3, 5-OCH_3), 6.23 (br, 2 H, NH_2, exch), 7.11–7.21 (m, 2 H, Ar), 7.28–7.31 (m, 2 H, Ar), 8.08–8.10 (m, 1 H, Ar), 8.15 (s, 1 H, 4-NH, exch), 11.29 (s, 1 H, 9-NH, exch). HRMS (ESI) calcd. for $C_{19}H_{19}N_5O_3$ $(M+H)^+$: 365.1561, found: 365.1543.

***N*^{4}-Methyl-*N*^{4}-(4-methylphenyl)-9*H*-pyrimido[4,5-*b*]indole-2,4-diamine (13)—**Using the general procedure described above, the reaction of **21** (100 mg, 0.33 mmol) with *N*,4-dimethylaniline **28** (300 mg, 2.47 mmol) and 3 drops of conc. HCl for 18 h afforded **13** in 71% yield. TLC R_f 0.12 (chloroform-methanol 15:1 with 2 drops concentrated NH_4OH); mp 252.7–253.5 °C; ^{1}H NMR (DMSO-d^6) δ 2.27 (s, 3 H, CH_3), 3.53 (s, 3 H, NCH_3), 5.79–5.81 (m, 1 H, Ar), 6.25 (br, 2 H, NH_2, exch), 6.52–6.56 (m, 1 H, Ar), 6.95–6.99 (m, 1 H, Ar), 7.07–7.17 (m, 5 H, Ar), 11.26 (s, 1 H, 9-NH, exch). HRMS (ESI) calcd. for $C_{18}H_{17}N_5$ $(M+H)^+$: 304.1557, found: 304.1539.

***N*^{4}-Ethyl-*N*^{4}-(4-methoxyphenyl)-9*H*-pyrimido[4,5-*b*]indole-2,4-diamine (14)—**Using the general procedure described above, the reaction of **21** (80 mg, 0.26 mmol) with *N*-ethyl-4-methoxyaniline **29** (120 mg, 0.78 mmol) and 1 drop of conc. HCl for 72 h afforded 30 mg of **14** as a white solid in 31% yield. TLC R_f 0.50 (chloroform-methanol 15:1); mp 223.9–224.6 °C; ^{1}H NMR (DMSO-d^6) δ 1.15–1.19 (t, 3 H, J = 6.9 Hz, CH_3), 3.74 (s, 3 H, *O*-CH_3), 4.09–4.13 (q, 2 H, J = 6.9 Hz, N^4-CH_2), 5.66–5.68 (d, 1 H, Ar), 6.15 (s, 2 H, 2-NH_2, exch), 6.50–6.54 (t, 1 H, Ar), 6.90–6.97 (m, 3 H, Ar), 7.12–7.16 (m, 3 H, Ar), 11.20 (s, 1 H, 9-NH, exch). Anal. calcd. for $C_{19}H_{19}N_5O \cdot 0.90\ CH_3OH$: C, 65.98; H, 6.29; N, 19.33; Found: C, 65.81; H, 6.15; N, 19.31.

***N*^{4}-(4-Ethoxyphenyl)-*N*^{4}-methyl-9*H*-pyrimido[4,5-*b*]indole-2,4-diamine (15)—**In a round bottom flask, compound **21** (80 mg, 0.26 mmol), 4-ethoxy-*N*-methylaniline **30** (120 mg, 0.78 mmol) and 1 drop of conc. HCl were heated to reflux in 30 mL isopropanol for 120 h. After cooling to rt, silica gel (500 mg) was added, and isopropanol was removed under reduced pressure. Purification was performed by column chromatography using 0.5% methanol in chloroform to provide 63 mg of **15** as a white solid in 71% yield. TLC R_f 0.43 (chloroform-methanol 15:1); mp 238.8–239.6 °C; ^{1}H NMR (DMSO-d^6) δ 1.29–1.32 (t, 3 H,

J = 6.9 Hz, CH_3), 3.50 (s, 3 H, N^4-CH_3), 3.97–4.02 (q, 2 H, J = 6.9 Hz, CH_2), 5.76–5.78 (d, 1 H, Ar), 6.22 (s, 2 H, 2-NH_2, exch), 6.53–6.57 (t, 1 H, Ar), 6.88–6.90 (m, 2 H, Ar), 6.95–6.98 (t, 1 H, Ar), 7.13–7.15 (m, 3 H, Ar), 11.24 (s, 1 H, 9-NH, exch). Anal. calcd. for $C_{19}H_{19}N_5O$: C, 68.45; H, 5.74; N, 21.01; Found: C, 68.40; H, 5.61; N, 21.01.

***N*-Ethyl-4-methoxyaniline (29)—**4-methoxyaniline **31** (246.3 mg, 2.0 mmol), triethylamine (303.57 mg, 0.42 mL, 3 mmol), 10% Pd/C (32 mg, 0.03 mmol, 1.5 mol% relative to **31**), and dry toluene (2.5 mL) were added to an argon-filled 2–5 mL biotage microwave vial. The vial was sealed, and the reaction was run in a microwave at 175 °C for 1.5 h. The reaction vessel was cooled to room temperature, and the palladium catalyst was removed by filtration through celite and washed with ethyl acetate. Silica gel (1 g) was added, and the solvent was removed under reduced pressure. Purification was performed by column chromatography with hexane/ethyl acetate (95/5) to afford *N*-ethyl-4-methoxyaniline **29** as a pale yellow liquid (211.69 mg, 70%). The analytical values agree well with the literature.[19] TLC R_f 0.61 (hexane-ethyl acetate 1:1); ^{1}H NMR ($CDCl_3$) δ 1.26–1.29 (t, 3 H, J = 7.1 Hz, CH_3), 3.12–3.17 (q, 2 H, J = 7.1 Hz, *N*-CH_2), 3.79 (s, 3 H, 4-OCH_3), 6.62–6.64 (m, 2 H, Ar), 6.82–6.84 (m, 2 H, Ar).

4-Ethoxy-*N*-methylaniline (30)

To a solution of sodium methoxide (540.2 mg, 10 mmol) in 5 mL of methanol in a 25 mL round bottom flask was added 4-ethoxyaniline **32** (274.36 mg, 2 mmol). The resultant solution was then added to a 100 mL round bottom flask containing paraformaldehyde (84.08 mg, 2.8 mmol) in 5 mL of methanol. The reaction mixture was stirred at room temperature under argon atmosphere. After 5 h, sodium borohydride (121.02 mg, 2 mmol) was added, and the reaction mixture was heated to reflux for 2 h. After cooling to rt, silica gel (1 g) was added, and the solvent was removed in vacuo. The resultant plug was purified using column chromatography with hexane/ethyl acetate (95/5) to afford 4-ethoxy-*N*-methylaniline **30** as a light brown liquid (227.6 mg, 75%). The analytical values agree well with the literature.[20] TLC R_f 0.6 (hexane-ethyl acetate 1:1); ^{1}H NMR ($CDCl_3$) δ 1.43–1.46 (t, 3 H, J = 7.0 Hz, CH_3), 2.82 (s, 3 H, *N*-CH_3), 3.56 (s, 1 H, NH), 3.99–4.04 (q, 2 H, J = 7.0 Hz, *O*-CH_2), 6.61–6.63 (m, 2 H, Ar), 6.86–6.88 (m, 2 H, Ar).

Cellular studies

Cell culture

A-10, SK-OV-3 and HeLa cells were purchased directly from the American Type Culture Collection (Manassas, VA). A-10 cells are rat aortic smooth muscle cells, SK-OV-3 human ovarian carcinoma cells and HeLa, human cervical carcinoma cells. MDA-MB-435 human melanoma cells were obtained from the Lombardi Cancer Center, Georgetown University. The SK-OV-3 MDR-1-6/6 and HeLa WTβIII cell lines have been previously described.[23]

Evaluation of cellular microtubule effects

The effects of the compounds on microtubules were evaluated in A-10 cells using a β-tubulin antibody and indirect immunofluorescence techniques. The EC_{50}, the concentration required to cause 50% loss of interphase microtubules was calculated from at least 3 independent experiments.[32] The EC_{50} for each experiment was calculated and the numbers represent the mean ±SD.

Antiproliferative effects

The sulforhodamine B (SRB) assay[21, 22] was used to measure the antiproliferative and cytotoxic effects of the compounds.[23] The IC_{50} represents the mean of 3–5 independent experiments.

Preliminary study of inhibition of tubulin polymerization

Inhibition of tubulin polymerization was measured turbidimetrically by absorbance at 340 nm. The assays utilized 2.5 mg/mL purified porcine brain tubulin incubated with tubulin assembly buffer (80 mM Na-Pipes, pH 6.9, 1 mM EGTA, 1 mM $MgCl_2$, 1 mM GTP and 10% glycerol) with vehicle or compounds indicated in a final volume of 100 μL. Tubulin polymerization was monitored at 37 °C in a Spectromax Plus 96 well plate spectrophotometer (Molecular Devices).

Cell cycle analysis

MDA-MB-435 cells were treated for 18 h with vehicle, **6** or 12.5 nM paclitaxel as a positive control. Following drug treatment, the cells were harvested and stained with Krishan's reagent[33] and analyzed using a FacsCalibur flow cytometer. The data are plotted as propidium iodide intensity versus the number of events.

Reagents

Paclitaxel was purchased from Sigma-Aldrich (St. Louis, MO) and CA-4 used in the cellular studies was synthesized by Dr. Doug Frantz of the University of Texas San Antonio.

Quantitative tubulin studies

The purification of electrophoretically homogeneous tubulin from bovine brains was described previously.[25] Inhibition of assembly was performed as described in detail previously,[26] using 10 μM (1.0 mg/mL) tubulin and various compound concentrations. The GTP (0.4 mM) was added to reaction mixtures following a 15 min preincubation at 30 °C. The parameter measured to obtain IC_{50} values was the extent of assembly after 20 min at 30 °C. Measurement of inhibition of colchicine binding was measured as described in detail previously.[27] Reaction mixtures contained 1.0 μM tubulin, 5.0 μM [^{3}H]colchicine, obtained from Perkin-Elmer, and 5.0 μM inhibitor, with incubation for 10 min at 37 °C. CA-4 was generously provided by Dr. G. A. Pettit of Arizona State University, Tempe AZ.

Supplementary Material

Refer to Web version on PubMed Central for supplementary material.

Acknowledgments

This work was supported, in part, by the National Institutes of Health and National Cancer Institute Grant CA142868 (AG and SLM) and the Duquesne University Adrian Van Kaam Chair in Scholarly Excellence (AG). We acknowledge support from the CTRC Cancer Center Support Grant, CCSG (CA054174) (SLM).

Abbreviations

CA-4	Combretastatin A-4
MDR	multidrug resistance
Pgp	P-glycoprotein
Rr	Relative resistance

DAMA colchicine *N*-deacetyl-*N*-(2-mercaptoacetyl)colchicine

References

1. Gangjee, A.; Zaware, N.; Devambatla, RKV.; Mooberry, SL.; Hamel, E. From Abstracts of Papers. 242nd ACS National Meeting & Exposition; August 28–September 1, 2011; Denver, CO, United States. 2011. MEDI-53.
2. Stanton RA, Gernert KM, Nettles JH, Aneja R. Drugs that target dynamic microtubules: A new molecular perspective. Med. Res. Rev. 2011; 31:443–481. [PubMed: 21381049]
3. Dumontet C, Jordan MA. Microtubule-binding agents: A dynamic field of cancer therapeutics. Nat. Rev. Drug Discov. 2010; 9:790–803. [PubMed: 20885410]
4. Komlodi-Pasztor E, Sackett D, Wilkerson J, Fojo T. Mitosis is not a key target of microtubule agents in patient tumors. Nat. Rev. Clin. Oncol. 2011; 8:244–250. [PubMed: 21283127]
5. Jordan A, Hadfield JA, Lawrence NJ, McGown AT. Tubulin as a target for anticancer drugs: agents which interact with the mitotic spindle. Med. Res. Rev. 1998; 18:259–296. [PubMed: 9664292]
6. Correia JJ, Lobert S. Physiochemical aspects of tubulin-interacting antimitotic drugs. Curr. Pharm. Des. 2001; 7:1213–1228. [PubMed: 11472263]
7. Siemann DW, Chaplin DJ, Walicke PA. A review and update of the current status of the vasculature-disabling agent combretastatin-A4 phosphate (CA4P). Expert Opin. Investig. Drugs. 2009; 18:189–197. Ng QS, Goh V, Carnell D, Meer K, Padhani AR, Saunders MI, Hoskin PJ. Tumor antivascular effects of radiotherapy combined with combretastatin A4 phosphate in human non-small-cell lung cancer. Int. J. Radiation Oncology Biol. Phys. 2007; 67:1375–1380. c. Selected clinical trials data for CA4P either alone or in combination: http://www.oxigene.com/pipeline/zybrestat_in_oncology/; Combretastatin A4 phosphate in treating patients with advanced solid tumors, http://clinicaltrials.gov/ct2/show/NCT00003768?term=CA4P&rank=11; Combretastatin A4 phosphate in treating patients with advanced anaplastic thyroid cancer, http://clinicaltrials.gov/ct2/show/NCT00060242?term=CA4P&rank=9; A safety and efficacy study of carboplatin, paclitaxel, bevacizumab and CA4P in non-small cell lung cancer (FALCON), http://clinicaltrials.gov/ct2/show/NCT00653939?term=combretastatin&rank=8.
8. Clinical trials: A phase I clinical trial of OXi4503 for relapsed and refractory AML and MDS, http://clinicaltrials.gov/ct2/show/NCT01085656?term=CA1P&rank=1.
9. Fojo AT, Menefee M. Microtubule targeting agents: basic mechanisms of multidrug resistance (MDR). Semin. Oncol. 2005; 32:S3–S8. [PubMed: 16360716]
10. Kumar N. Taxol-induced polymerization of purified tubulin. Mechanism of action. J. Biol. Chem. 1981; 256:10435–10441. [PubMed: 6116707]
11. Leonard GD, Fojo T, Bates SE. The role of ABC transporters in clinical practice. Oncologist. 2003; 8:411–424. [PubMed: 14530494]
12. Lhomme C, Joly F, Walker JL, Lissoni AA, Nicoletto MO, Manikhas GM, Baekelandt MMO, Gordon AN, Fracasso PM, Mietlowski WL, Jones GJ, Dugan MH. Phase III study of valspodar (PSC 833) combined with paclitaxel and carboplatin compared with paclitaxel and carboplatin alone in patients with stage IV or suboptimally debulked stage III epithelial ovarian cancer or primary peritoneal cancer. J. Clin. Oncol. 2008; 26:2674–2682. [PubMed: 18509179]
13. Fromm MF. P-glycoprotein: A defense mechanism limiting oral bioavailability and CNS accumulation of drugs. Int. J. Clin. Pharmacol. Ther. 2000; 38:69–74. [PubMed: 10706193]
14. Kavallaris M, Kuo DY, Burkhart CA, Regl DL, Norris MD, Haber M, Horwitz SB. Taxol-resistant epithelial ovarian tumors are associated with altered expression of specific beta-tubulin isotypes. J. Clin. Invest. 1997; 100:1282–1293. [PubMed: 9276747]
15. Hari M, Yang H, Zeng C, Canizales M, Cabral F. Expression of class III beta-tubulin reduces microtubule assembly and confers resistance to paclitaxel. Cell Motil. Cytoskeleton. 2003; 56:45–56. [PubMed: 12905530]
16. Seve P, Dumontet C. Is class III β-tubulin a predictive factor in patients receiving tubulin-binding agents? Lancet Oncol. 2008; 9:168–175. [PubMed: 18237851]

17. Gangjee A, Zhao Y, Lin L, Raghavan S, Roberts EG, Risinger AL, Hamel E, Mooberry SL. Synthesis and discovery of water-soluble microtubule targeting agents that bind to the colchicine site on tubulin and circumvent Pgp mediated resistance. J. Med. Chem. 2010; 53:8116–8128. [PubMed: 20973488]
18. Gangjee A, Patel J, Kisliuk RL, Gaumont Y. 5,10-Methylenetetrahydro-5-deazafolic acid and analogs: Synthesis and biological activities. J. Med. Chem. 1992; 35:3678–3685. [PubMed: 1433179]
19. Lubinu MC, De Luca L, Giacomelli G, Porcheddu A. Microwave-promoted selective mono-N-alkylation of anilines with tertiary amines by heterogeneous catalysis. Chem. Eur. J. 2011; 17:82–85. [PubMed: 21207602]
20. Abdel-Magid AF, Carson KG, Harris BD, Maryanoff CA, Shah RD. Reductive amination of aldehydes and ketones with sodium triacetoxyborohydride. Studies on direct and indirect reductive amination procedures. J. Org. Chem. 1996; 61:3849–3862. [PubMed: 11667239]
21. Skehan P, Storeng R, Scudiero D, Monks A, McMahon J, Vistica D, Warren JT, Bokesch H, Kenney S, Boyd MR. New colorimetric cytotoxicity assay for anticancer-drug screening. J. Natl. Cancer Inst. 1990; 82:1107–1112. [PubMed: 2359136]
22. Boyd MR, Paull KD. Some practical considerations and applications of the National Cancer Institute in vitro anticancer drug discovery screen. Drug Dev. Res. 1995; 34:91–109.
23. Risinger AL, Jackson EM, Polin LA, Helms GL, LeBoeuf DA, Joe PA, Hopper-Borge E, Luduena RF, Kruh GD, Mooberry SL. The taccalonolides: Microtubule stabilizers that circumvent clinically relevant taxane resistance mechanisms. Cancer Res. 2008; 68:8881–8888. [PubMed: 18974132]
24. We thank the NCI for providing the tumor cell growth inhibitory activity for **6** in the NCI 60 cell line panel.
25. Hamel E, Lin CM. Separation of active tubulin and microtubule-associated proteins by ultracentrifugation and isolation of a component causing the formation of microtubule bundles. Biochemistry. 1984; 23:4173–4184. [PubMed: 6487596]
26. Hamel E. Evaluation of antimitotic agents by quantitative comparisons of their effects on the polymerization of purified tubulin. Cell Biochem. Biophys. 2003; 38:1–21. [PubMed: 12663938]
27. Verdier-Pinard P, Lai J-Y, Yoo H-D, Yu J, Marquez B, Nagle DG, Nambu M, White JD, Falck JR, Gerwick WH, Day BW, Hamel E. Structure-activity analysis of the interaction of curacin A, the potent colchicine site antimitotic agent, with tubulin and effects of analogs on the growth of MCF-7 breast cancer cells. Mol. Pharmacol. 1998; 53:62–76. [PubMed: 9443933]
28. Ravelli RBG, Gigant B, Curmi PA, Jourdain I, Lachkar S, Sobel A, Knossow M. Insight into tubulin regulation from a complex with colchicine and a stathmin-like domain. Nature. 2004; 428:198–202. [PubMed: 15014504]
29. Molecular Operating Environment (MOE 2008.10). Montreal, Quebec, Canada: Chemical Computing Group, Inc.; 2008. www.chemcomp.com.
30. Nguyen TL, McGrath C, Hermone AR, Burnett JC, Zaharevitz DW, Day BW, Wipf P, Hamel E, Gussio R. A common pharmacophore for a diverse set of colchicine site inhibitors using a structure-based approach. J. Med. Chem. 2005; 48:6107–6116. [PubMed: 16162011]
31. Taylor EC, Cocuzza AJ. Synthesis and properties of 7-azaxanthopterin. J. Org. Chem. 1979; 44:1125–1128.
32. Lee L, Robb LM, Lee M, Davis R, Mackay H, Chavda S, Babu B, O'Brien EL, Risinger AL, Mooberry SL, Lee M. Design, Synthesis, and Biological Evaluations of 2,5-Diaryl-2,3-dihydro-1,3,4-oxadiazoline Analogs of Combretastatin-A4. J. Med. Chem. 2010; 53:325–334. [PubMed: 19894742]
33. Krishan A. Rapid flow cytofluorometric analysis of mammalian cell cycle by propidium iodide. J. Cell Biol. 1975; 66:188–193. [PubMed: 49354]

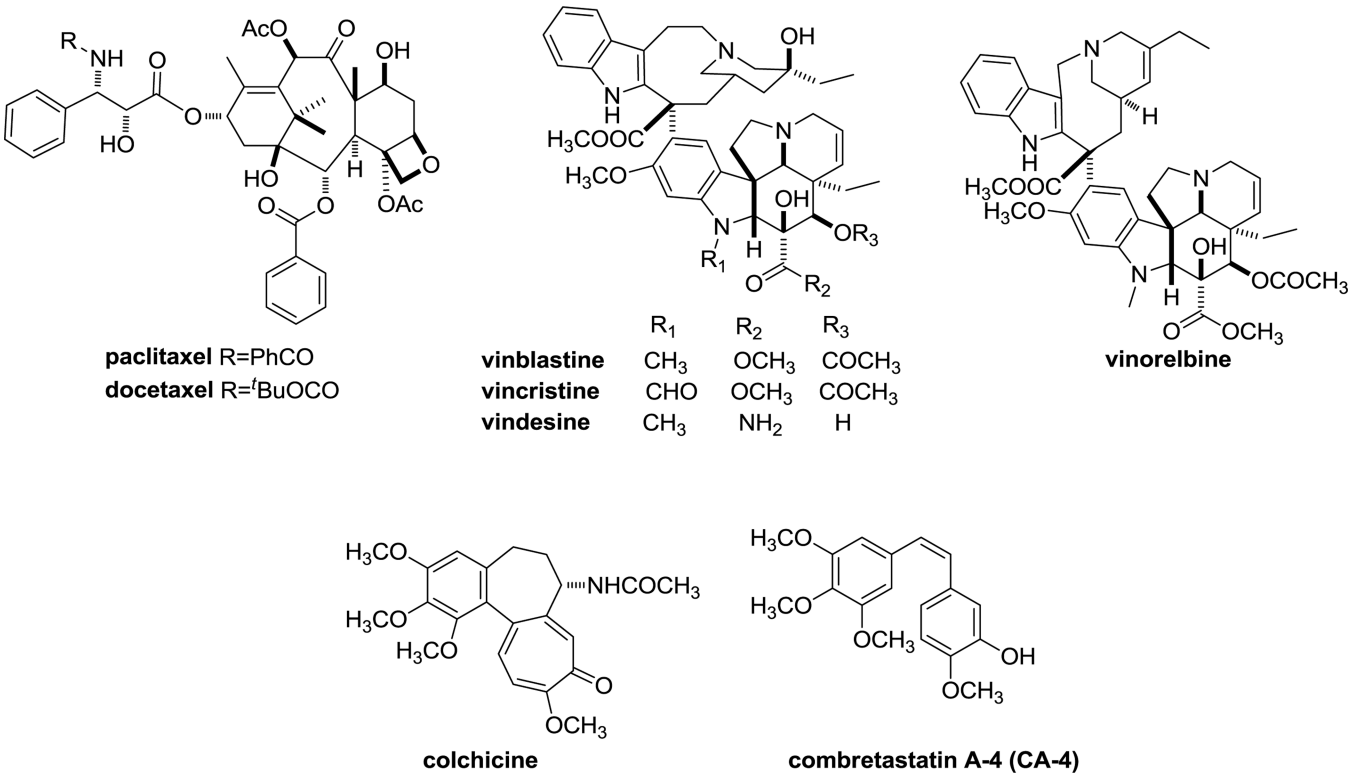

Figure 1.
Tubulin binding agents.

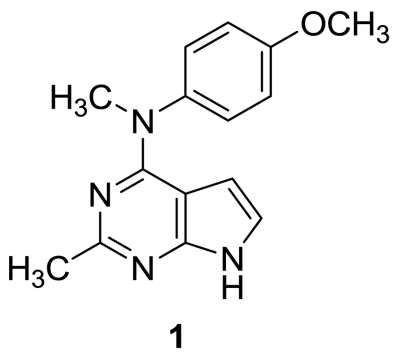

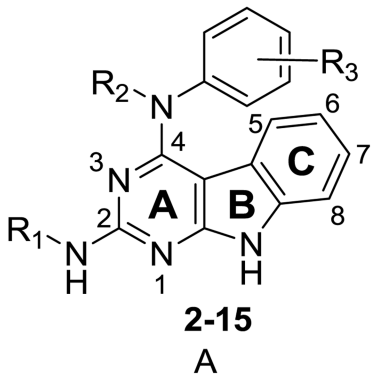

	R_1	R_2	R_3
2	H	H	3'-OMe
3	Piv	H	3'-OMe
4	H	H	4'-OMe
5	Piv	H	4'-OMe
6	H	Me	4'-OMe
7	Piv	Me	4'-OMe
8	H	H	3'-Br
9	Piv	H	3'-Br
10	H	Me	3'-OMe
11	Piv	Me	3'-OMe
12	H	H	3',4',5'-triOMe
13	H	Me	4'-Me
14	H	Et	4'-OMe
15	H	Me	4'-OEt

Figure 2.
Parent pyrrolo[2,3-*d*]pyrimidine **1** and target pyrmido[4,5-*b*]indoles **2–15**.

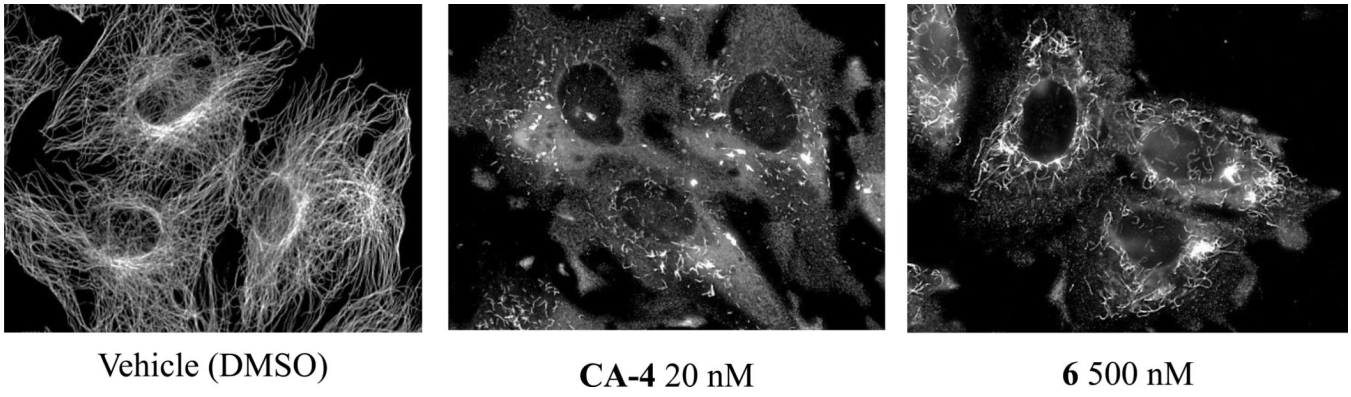

Figure 3.

The effects of vehicle, CA-4 or **6** on interphase microtubules. A-10 cells were treated with vehicle, 20 nM CA-4 or 500 nM **6**. Following 18 h incubation, the cells were fixed with cold methanol and microtubules were visualized by indirect immunofluorescence techniques with a β-tubulin antibody.

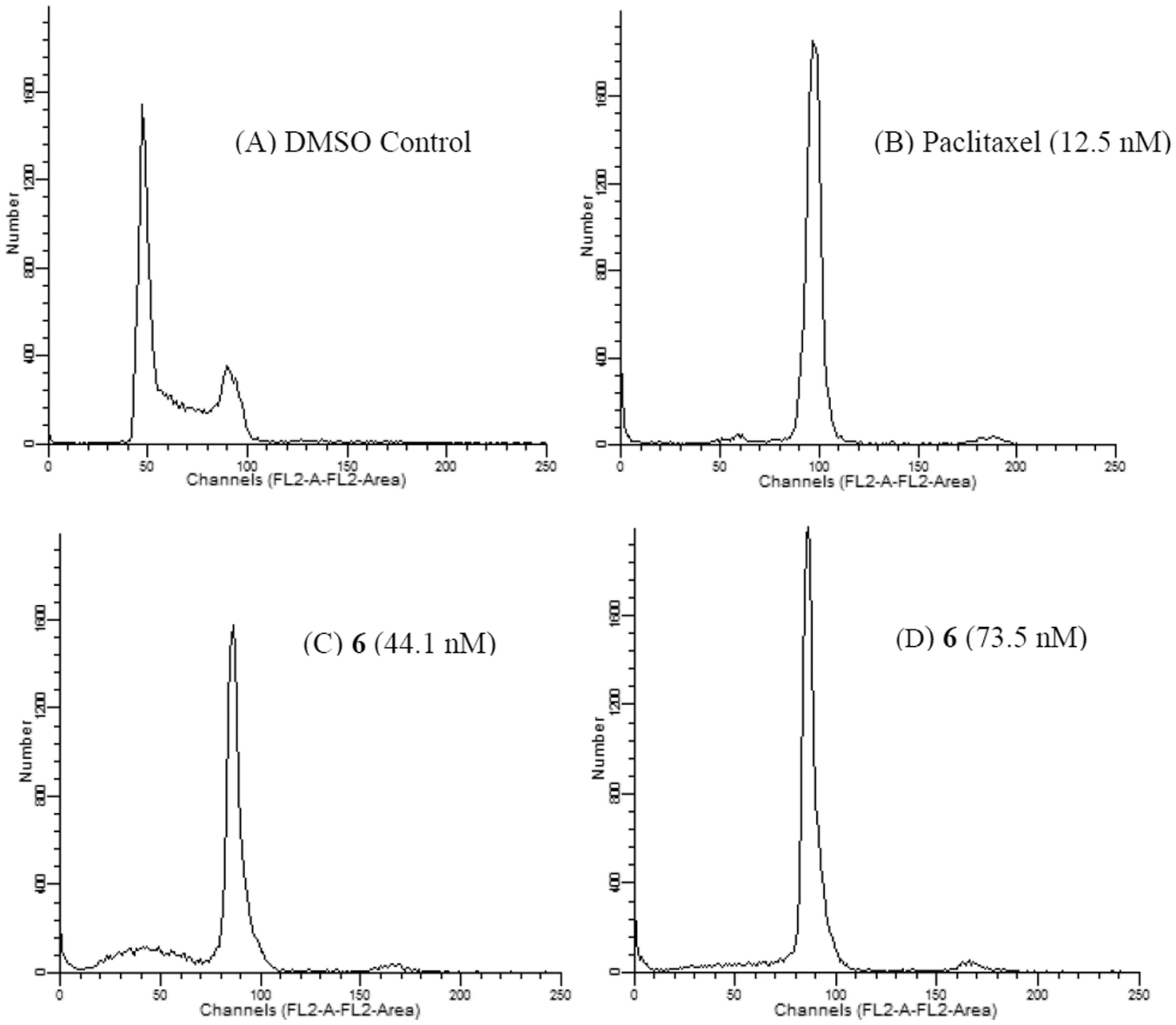

Figure 4.

The effects of **6** on cell cycle distribution. MDA-MD-435 cells were treated with vehicle (A), 12.5 nM paclitaxel (6.5 × IC_{50} for inhibition of proliferation) (B), 44.1 nM **6** (3 × IC_{50}) (C), or 73.5 nM **6** (5 × IC_{50}) (D) for 18 h. The cells were harvested and stained with propidium iodide, and cell cycle distribution was evaluated using flow cytometry.

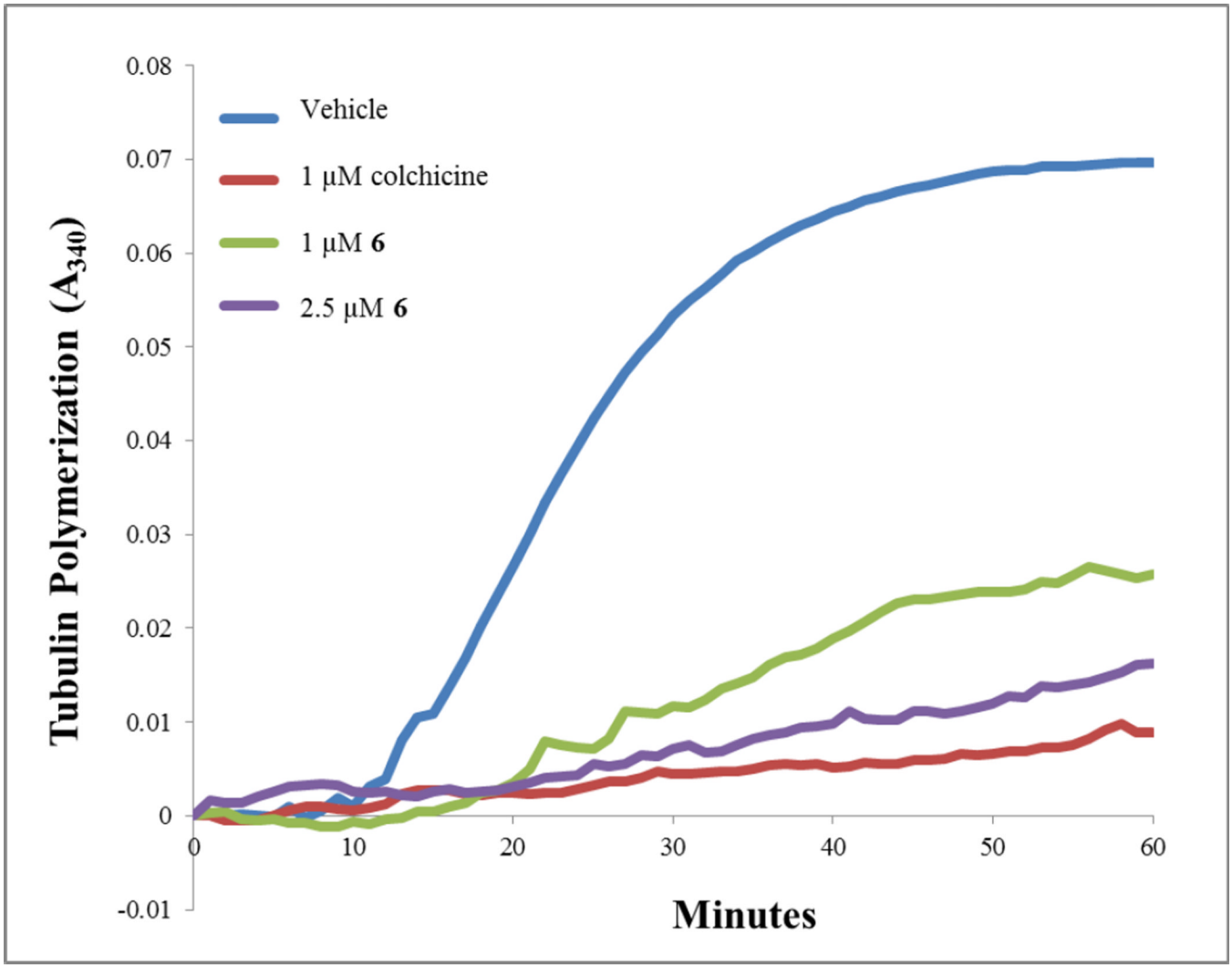

Figure 5.

Effects of **6** on tubulin assembly. Porcine brain tubulin, 2.5 mg/mL (Cytoskeleton Inc, Denver CO), was incubated with **6**, colchicine or DMSO vehicle in general tubulin buffer containing 10% glycerol and 1 mM GTP. The effects of these drugs on tubulin polymerization were monitored by measuring the absorbance at 340 nm at 37 °C in a 96 well Spectromax Plus spectrophotometer (Molecular Devices).

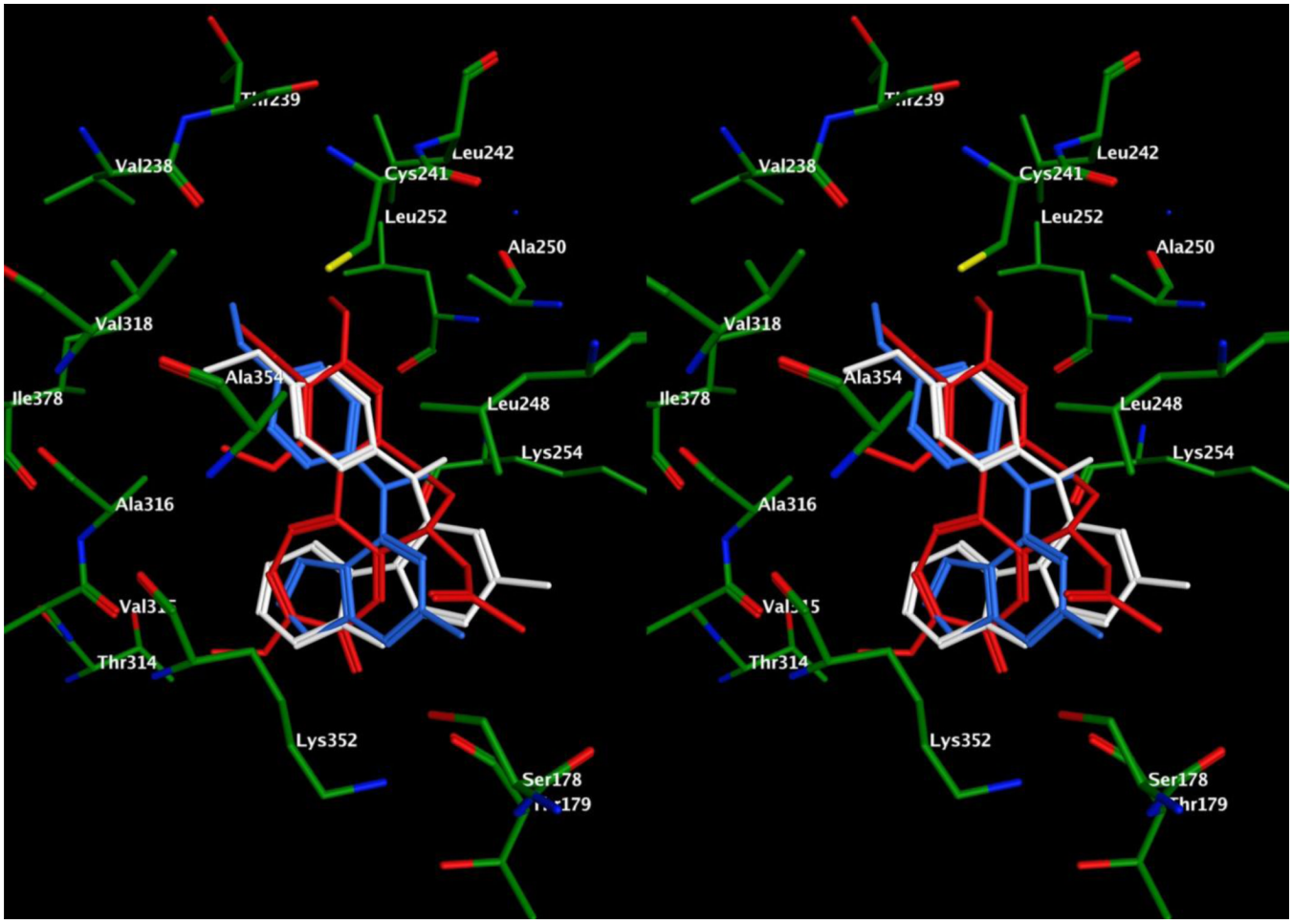

Figure 6.
Stereo view. Superimposition of docked poses of **6** (white) and **1** (blue) overlaid with DAMA colchicine (red) in the colchicine site of tubulin.

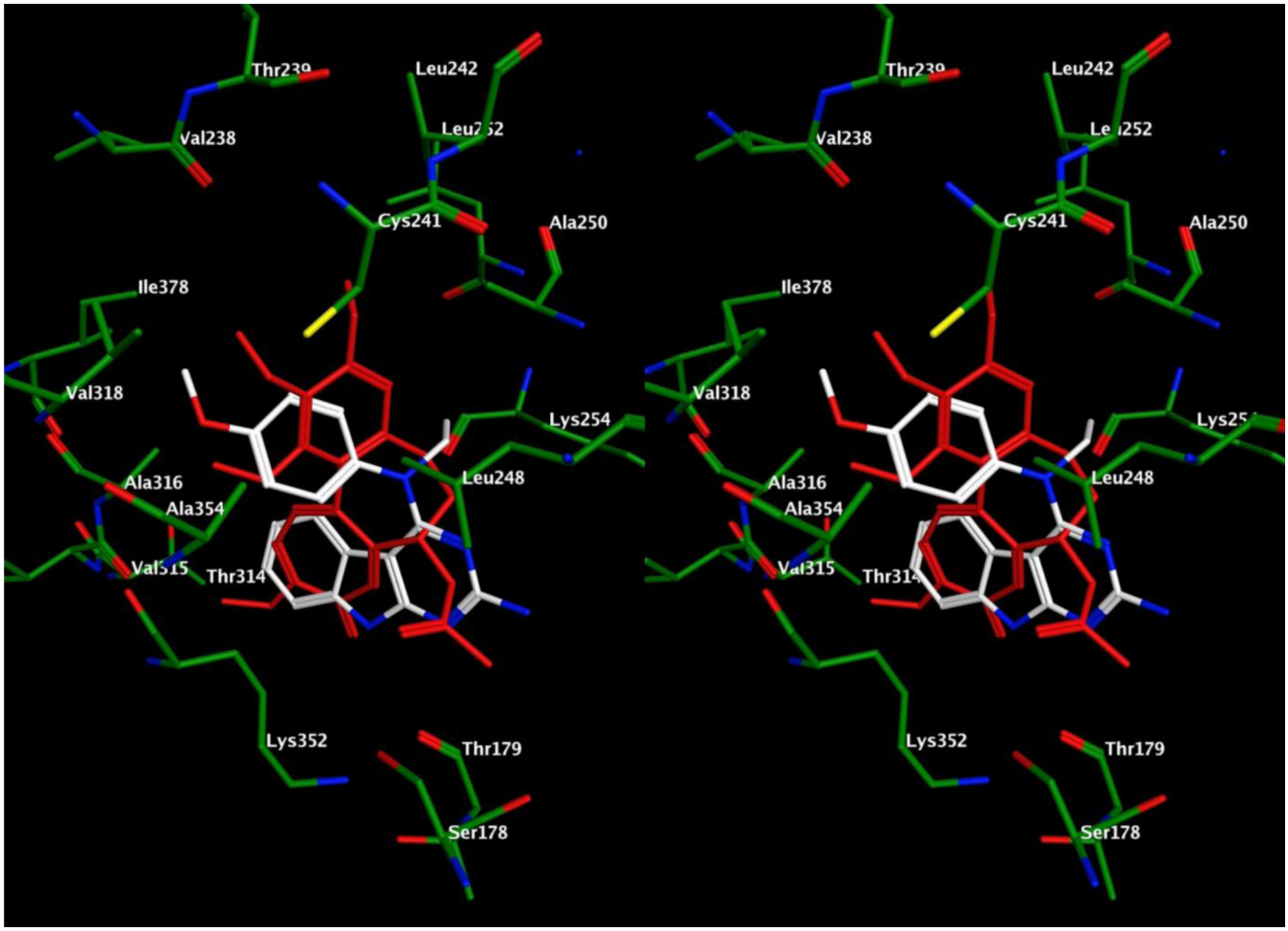

Figure 7.
Stereo view. Superimposition of docked poses of **14** (white) overlaid with DAMA colchicine (red) in the colchicine site of tubulin.

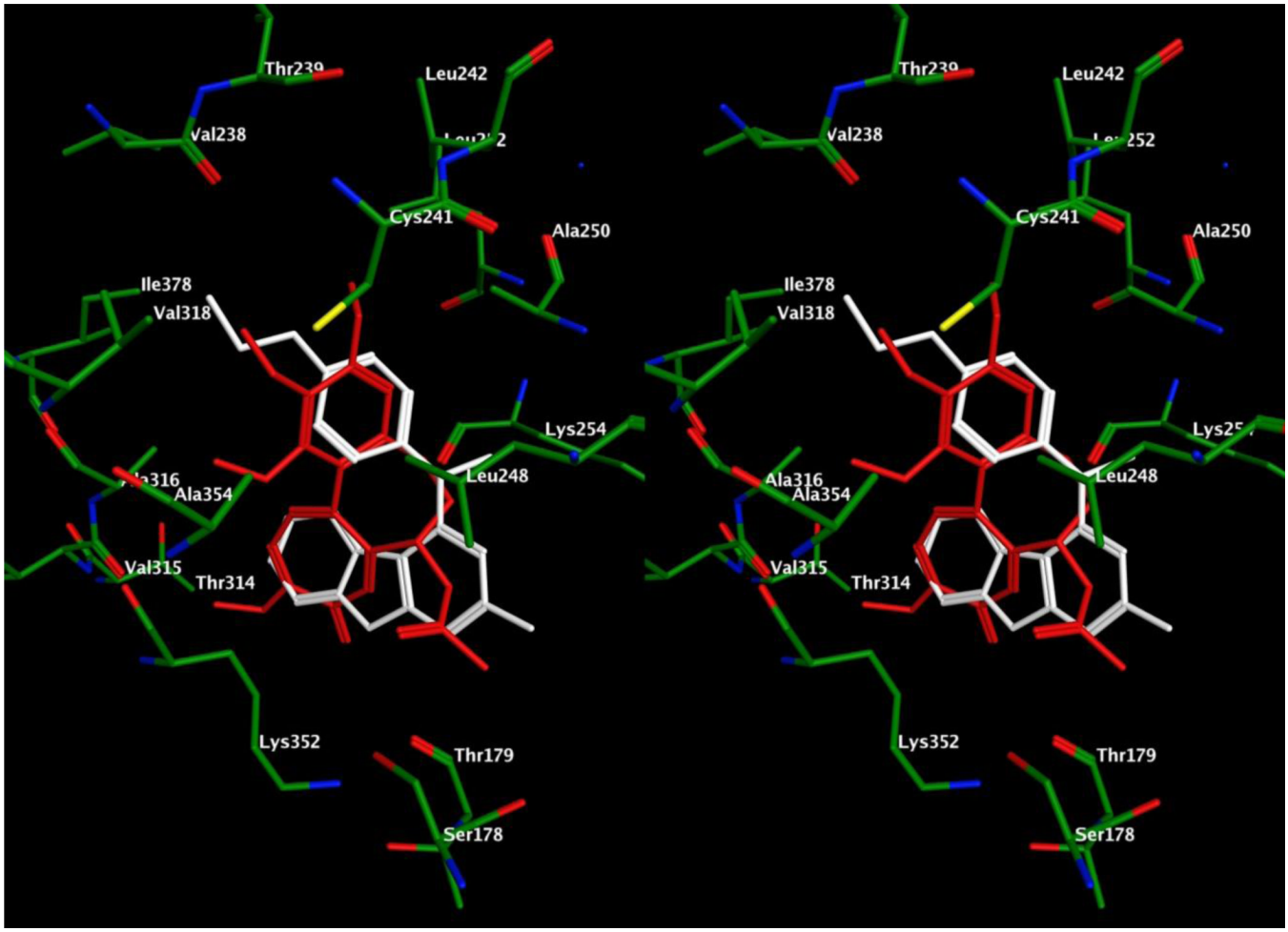

Figure 8.
Stereo view. Superimposition of docked poses of **15** (white) overlaid with DAMA colchicine (red) in the colchicine site of tubulin.

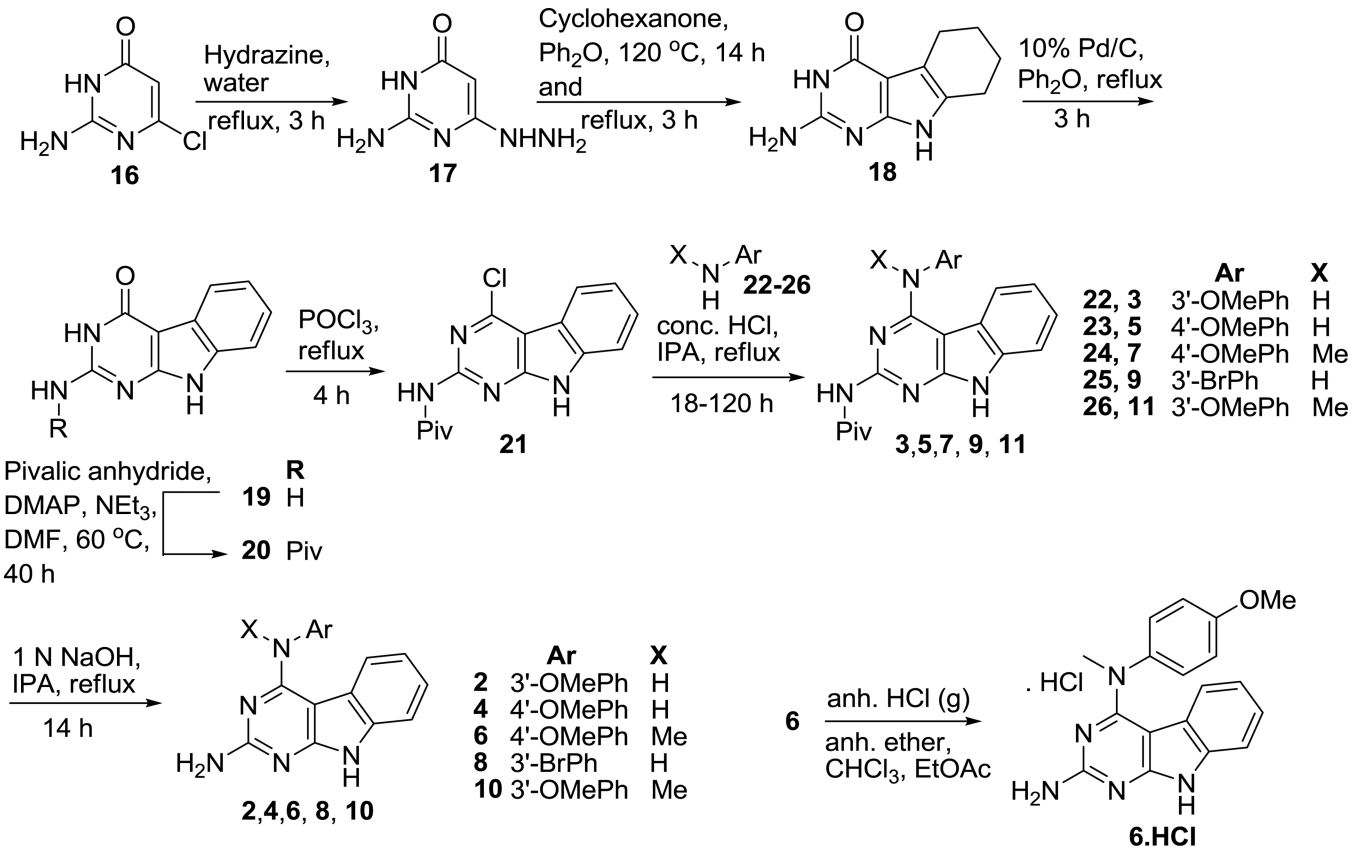

Scheme 1.
Synthesis of compounds **2–11** and **6·HCl**

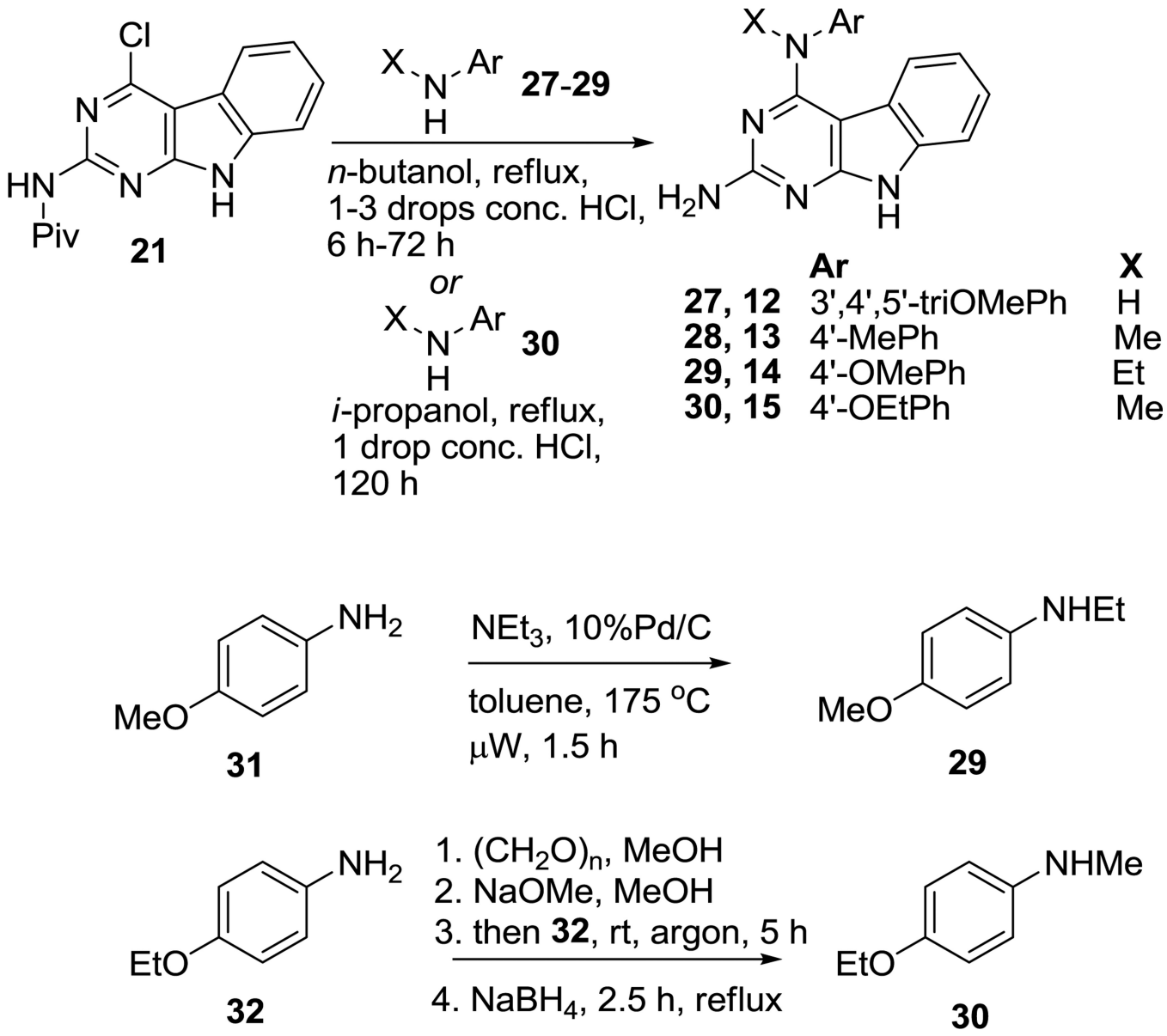

Scheme 2.
Synthesis of compounds **12–15**

Table 1

IC_{50} Values for the Ability of the Compounds to Inhibit Proliferation of MDA-MB-435 Cells and EC_{50} Values for Loss of Cellular Microtubules.

Compd	IC_{50} ± SD (nM) (MDA-MB-435)	EC_{50} for Microtubule Depolymerization in A-10 cells (nM)	EC_{50} /IC_{50}
2	ND[a]	> 40 μM	ND[a]
3	ND[a]	> 40 μM	ND[a]
4	ND[a]	> 40 μM	ND[a]
5	ND[a]	> 40 μM	ND[a]
6	14.7 ± 1.5	105 ± 12	7.1
7	ND[a]	> 40 μM	ND[a]
8	ND[a]	> 40 μM	ND[a]
9	ND[a]	> 40 μM	ND[a]
10	ND[a]	> 40 μM	ND[a]
11	ND[a]	> 40 μM	ND[a]
12	ND[a]	> 10 μM	ND[a]
13	ND[a]	> 10 μM	ND[a]
14	23.5 ± 1.2	198 ± 8	8.4
15	14.4 ± 0.5	83 ± 4	6.5
1[b]	183 ± 3.4	5800	31.7
CA-4[c]	3.4 ± 0.6	13	3.8

[a] ND: Not determined.

[b] Results previously published.[17]

[c] Results previously published.[23] The IC_{50} values were obtained in 3–5 independent experiments each utilizing triplicate or quadruplicate wells for each concentration and are expressed ± SD. The EC_{50} values were obtained in 3–4 experiments, each evaluating a large range of concentrations of each compound and are expressed ± SD.

Bioorg Med Chem. Author manuscript; available in PMC 2014 February 15.

Table 2

Human Cancer Cell Growth Inhibitory Activity GI_{50} (nM) of **6** in NCI 60 Cell Line Panel.

Panel/ Cell line	GI_{50} (nM) Compd 6	Panel/ Cell line	GI_{50} (nM) Compd 6	Panel/ Cell line	GI_{50} (nM) Compd 6	Panel/ Cell line	GI_{50} (nM) Compd 6
Leukemia		**Colon Cancer**		**Melanoma**		**Renal Cancer**	
CCRF-CEM	41.1	COLO 205	25.8	LOX IMVI	68.4	786 - 0	49.0
HL-60(TB)	32.2	HCC-2998	23.6	MALME-3M	304	A498	15.8
K-562	< 10	HCT-116	29.8	M14	16.6	ACHN	89.6
MOLT-4	47.7	HCT-15	26.1	MDA-MB-435	<10	CAKI-1	34.0
RPMI-8226	41.1	HT29	31.0	SK-MEL-2	19.7	RXF 393	16.9
SR	< 10	KM12	13.2	SK-MEL-28	< 10	SN12C	80.1
NSCLC		SW-620	19.0	SK-MEL-5	32.3	TK10	56.2
A549/ATCC	36.4	**CNS Cancer**		UACC-62	27.0	UO-31	53.7
EKVX	16.7	SF-268	37.7	**Ovarian cancer**		**Prostate Cancer**	
HOP-62	40.0	SF-295	26.0	IGROVI	34.0	PC-3	44.3
HOP-92	242	SF-539	24.2	OVCAR-3	12.9	DU-145	31.4
NCI-H226	133	SNB-19	50.9	OVCAR-4	52.7	**Breast Cancer**	
NCI-H23	31.8	SNB-75	12.7	OVCAR-5	51.2	MCF7	16.4
NCI-H322M	64.2	U251	37.3	OVCAR-8	42.3	MDA-MB-231/ATCC	64.6
NCI-H460	30.0			NCI/ADR-RES	11.5	HS 578T	11.5
NCI-H522	< 10			SK-OV-3	29.9	BT-549	94.5
						MDA-MB-468	26.9

Table 3

Compounds **6**, **14** and **15** are Effective in Cell Lines Expressing Pgp or βIII-tubulin

Compd	Effect of Pgp on drug sensitivity[b] IC_{50} ± SD (nM)			Effect of βIII-tubulin on drug sensitivity[c] IC_{50} ± SD (nM)		
	SK-OV-3	SK-OV-3 MDR-1-6/6	Rr[a]	HeLa	WT βIII	Rr[a]
6	27.6 ± 1.8	34.4 ± 5.9	1.2	21.3 ± 2.2	21.4 ± 3.5	1.0
1[d]	278 ± 19	435 ± 33	1.6	270 ± 26	186 ± 21	0.7
14	53.0 ± 1.9	72.0 ± 7.9	1.4	32.8 ± 0.8	45.5 ±1.0	1.4
15	23.0 ± 1.1	29.1 ± 1.7	1.3	23.1 ± 0.8	18.8 ± 0.5	0.8
paclitaxel	4.4 ± 0.6	2596 ± 119	590	1.6 ± 0.5	9.2 ± 0.2	5.8
CA-4	9.7± 0.2	11.5 ± 1.7	1.2	4.7 ± 1.1	5.2 ± 0.4	1.1

[a] Rr: Relative resistance.

[b] The SRB assay was used to evaluate the antiproliferative effects and determine the IC_{50} values of the compounds indicated. The SK-OV-3 MDR-1-6/6 cells were transduced with the *MDR-1* gene, and the sensitivity of this Pgp-expressing cell line was compared with the parental SK-OV-3 cells by dividing the IC_{50} of the Pgp overexpressing cell line by the IC_{50} of the parental cell line, yielding the Rr value.

[c] WT βIII cells were generated from HeLa cells by transfection with the βIII tubulin gene. The effects of the expression of βIII-tubulin on the sensitivity of the cell line pair were evaluated by calculating the Rr, by dividing the IC_{50} of the WT βIII cell line by the IC_{50} obtained in the parental HeLa cells.

[d] Results previously published.[17] The values were obtained from 3–5 independent experiments each using triplicate or quadruplicate points.

Table 4

Inhibition of Tubulin Assembly and Inhibition of Colchicine Binding.

Compd	Inhibition of tubulin assembly IC_{50} ± SD (μM)	Inhibition of colchicine binding (% inhibition ± SD) at 5 μM
6	1.4 ± 0.007	84 ± 0.5
14	1.7 ± 0.2	76 ± 3
15	1.7 ± 0.07	82 ± 1
1	2.6 ± 0.05	70 ± 2
CA-4	1.0 ± 0.09	99 ± 0.2

Inhibition of tubulin assembly was performed as described previously,[26] with tubulin at 10 μM (1.0 mg/mL) and varying concentrations of potential inhibitors. Extent of assembly at 20 min was the parameter measured. The CA-4 control is performed twice a year, and IC_{50} values obtained range from 1 to 1.2 μM. The most recent value is shown in the table. Inhibition of colchicine binding was performed as described previously,[27] with tubulin at 1.0 μM and both [^{3}H]colchicine and potential inhibitor at 5.0 μM. Incubation was for 10 min at 37 °C.